Nuclear Physics B90 (1975) 349–383
© North-Holland Publishing Company

K^-p CHARGE EXCHANGE AND HYPERON PRODUCTION CROSS SECTIONS FROM 860 TO 1000 MeV/c

M. JONES *, R. LEVI SETTI and D. MERRILL **
Department of Physics, Enrico Fermi Institute ‡,
University of Chicago, Chicago, Illinois 60615

R.D. TRIPP
Department of Physics, Lawrence Berkeley Laboratory ‡‡,
University of California, Berkeley, California 94720

Received 7 January 1975

The K^-p reactions leading to charge exchange and hyperon final states have been studied at nine momenta between 862 and 1001 MeV/c using data from a 600 000 picture exposure of the Lawrence Berkeley Laboratory 25" liquid hydrogen bubble chamber. Partial cross sections are determined for all final states resolved by kinematic fitting. In addition, differential cross sections are presented for the two-body final states $\bar{K}^0n$, $\Lambda\pi^0$ and $\Sigma^\pm\pi^\mp$ along with hyperon polarization angular distributions for $\Lambda\pi^0$ and $\Sigma^+\pi^-$.

1. Introduction

New data on the K^-p reactions leading to charge exchange and hyperon final states have been obtained at nine momenta between 862 and 1001 MeV/c in a collaborative effort between the University of Chicago and Lawrence Berkeley Laboratory (Chi-LBL collaboration). These data, which cover the c.m. energy range 1729–1794 MeV, represent ~4 times those obtained by the CERN-Heidelberg-Saclay (CHS) group [1] in this energy range. In the following sections, the new data presented include partial cross sections for all final states resolved by kinematic fitting; differential cross sections for $\bar{K}^0n$, $\Lambda\pi^0$, and $\Sigma^\pm\pi^\mp$; and hyperon polarization angular distributions for $\Lambda\pi^0$ and $\Sigma^+\pi^-$.

In the region chosen for investigation, many hyperon formation phenomena do occur for which clarification is needed. In addition to the well-established

* Now at Rutgers University, New Brunswick, New Jersey.
** Now at Lawrence Berkeley Laboratory, Berkeley, California.
‡ Research supported by the National Science Foundation.
‡‡ Research supported by the Atomic Energy Commission.

$\frac{5}{2}^-\Sigma(1765)$, a $\frac{1}{2}^-\Sigma(1750)$ has been reported but is still controversial in some of its properties [2]. Furthermore the reaction $K^-p \to \Sigma^0\eta$ reaches, from threshold, its maximum yield within the covered range. A detailed study of this effect, based on the present data, has already been presented [3]. Also reported [4,5] have been preliminary results of a partial wave analysis of the $\bar{K}N$, $\Sigma\pi$ and $\Lambda\pi$ channels in the 1700–1900 MeV energy interval, where our new material was incorporated with a comprehensive survey of data from the literature.

2. Exposure

An overall exposure of ~600 000 pictures, totalling ~6 events/μb, was obtained in the LBL 25″ Hydrogen Bubble Chamber at the Bevatron. The separated K^- beam [6] was tuned for nine nominal momentum values which covered the range from 870 to 1000 MeV/c with an estimated momentum bite of ±1% at each setting. The average number of tracks per frame ranged from 5 at the lowest momenta to 12 at the highest, where the beam intensity was sufficient to expose two frames per Bevatron pulse. The track bubble size was chosen to provide adequate contrast for measurement in the LBL Spiral Reader and to allow particle identification from ionization.

3. Scanning and measurement

All frames were scanned twice for the topologies 0-prong V^0, 2-prong V^{+0-}, 4-prong $V^{\pm}$ and τ-decays, yielding approximately 90 000 events. A conservative fiducial volume was adopted in the scan, and a restricted volume chosen after measurement for cross section determinations. The scanning efficiency for the events retained after the final fiducial cuts was better than 99% for all topologies. The events were measured and remeasured using the LBL Spiral Reader. Geometrical reconstruction and kinematic analysis were performed using the LBL SIOUX program sequence. The mass and momentum resolution obtained by this procedure will be illustrated with the presentation of the data in the following sections.

Kinematic ambiguities were, whenever feasible, resolved by visual observation of the track ionization. The numbers of identified events within the final fiducial volume and the processing failure rates for the various topologies are given in table 1. As usual, the events which failed were apportioned, for the purpose of cross-section determinations, according to the proportions of the various reactions observed among the successfully fitted events. It is important to note, however, that the events which failed were examined by physicists to check for biases and to eliminate spurious events. Therefore, we believe that any systematic errors due to these events are small and, in particular, that the numbers of τ decays, which are used in the cross-section normalizations, are very well determined.

Table 1
Number of events and failure rates for the various measured topologies

Topology	No. of events	Failure rate
τ	9939	5%
0-prong V^0	25538	4%
2-prong V^0	13347	5%
2-prong V^+	8448	5%
2-prong V^-	8308	5%
4-prong V^+	79	11%
4-prong V^-	35	23%
total	65694	5%

4. Beam momentum calibration, K^- path lengths and determinations of cross sections

The determination of the central values of the beam momenta for each of the nine nominal settings was obtained from the measurement and fitting of τ decays. The distributions of the fitted beam momenta, extrapolated to the entrance window of the bubble chamber, are plotted in fig. 1. The central value and the spread of each momentum distribution were determined by unfolding the measurement resolution and the correlation of the beam momentum with the y-coordinate (perpendicular to the beam direction and the magnetic field) at the entrance window.

A beam averaging procedure was then adopted in all kinematic fits, including τ decays. This consists in using, for each fit, the weighted average of the measured beam track curvature and the curvature corresponding to the central value of the beam momentum degraded to the interaction point. Events for which these values were inconsistent were rejected. Table 2 gives the average momentum and spread of the distribution (including the spread due to different positions in the chamber) obtained from τ decays which satisfied the beam-averaging and fiducial volume criteria. The energy parameters in this table therefore represent the average c.m. energy and energy spread at each setting. Also given in table 2 are the K^- path lengths in events/mb within the fiducial volume. The latter were determined using the following relation

$$\text{path length (events/mb)} = \frac{N_\tau c\tau P_{K^-} n}{R M_{K^-}} = \frac{N_\tau P_{K^-}}{2.061}, \tag{4.1}$$

where P_{K^-} is in GeV/c, N_τ is the number of observed τ decays, c is the speed of light, $\tau = 1.237 \times 10^{-8}$ sec, $M_{K^-} = 493.84$ MeV, $R = 0.0558$ (the branching fraction for τ decay) [7] and n, the number of hydrogen atoms/cm^3, is based on a liquid H_2 density [8] of 0.0603 g/cm^3.

Use of these values for the cross-section normalization, and of the corrections to be described in the following, yielded the partial cross sections listed in table 3.

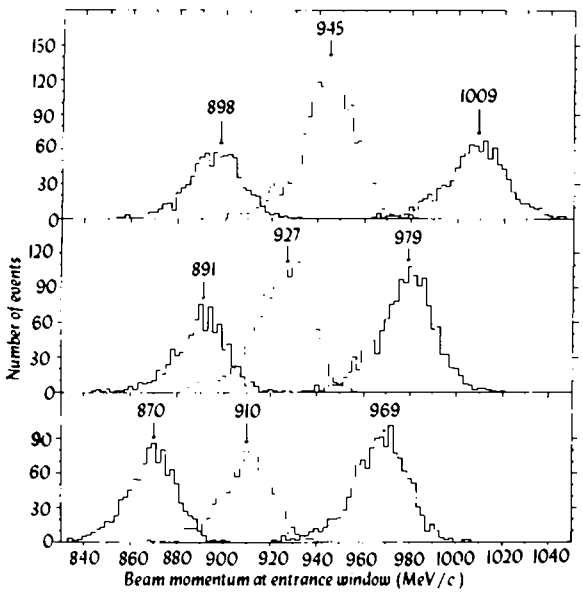

Fig. 1. Distributions of the fitted beam momenta from τ decay, reduced to the entrance window of the bubble chamber. Indicated are the central values in MeV/c.

Table 2
K^- path length

P_{K^-}(MeV/c)	$\sigma(P_{K^-})$	$E_{c.m.}$(MeV)	$\sigma(E_{c.m.})$	No. of τ	events/mb
862	8.2	1729	3.9	961	402
883	8.5	1739	4.0	796	341
888	8.5	1741	4.0	711	306
902	8.9	1748	4.2	916	401
918	8.8	1755	4.1	1385	616
936	8.7	1764	4.1	1684	764
960	8.6	1775	4.0	1238	576
971	9.0	1780	4.2	1358	639
1001	9.1	1794	4.3	890	432
total				9939	4477

Table 3
Partial cross sections (mb)

Final state	P_K - (MeV/c)								
	862	883	888	902	918	936	960	971	1001
0-prong K^0	5.34	5.41	5.69	6.03	5.47	6.16	6.99	7.63	9.10
	.29	.32	.35	.32	.24	.24	.30	.30	.42
$\bar{K}^0 n$	4.79	4.75	4.98	5.10	4.56	5.30	5.89	6.57	7.84
	.27	.30	.32	.29	.22	.22	.27	.27	.38
0-prong Λ	6.10	5.91	6.41	6.76	6.43	6.59	7.10	7.26	7.35
	.26	.28	.32	.29	.23	.21	.26	.25	.31
$\Lambda\gamma^0$	3.55	3.41	3.88	3.89	3.66	3.60	3.75	3.87	3.40
	.22	.21	.23	.21	.17	.16	.18	.18	.20
$\Sigma^0\gamma^0$	.99	.85	.82	.78	.75	.76	.81	.85	.99
EDPWA									
$\Lambda\eta$	.19	.13	.01	.10	.18	.11	.14	.12	.22
	.07	.07	.07	.07	.05	.05	.06	.05	.07
$\bar{K}^0 p\pi^-$	.16	.22	.22	.18	.25	.33	.41	.48	.51
	.04	.05	.05	.04	.04	.04	.05	.05	.07
$\Lambda\pi^+\pi^-$	3.60	3.76	3.75	4.07	3.85	3.63	3.85	4.32	4.66
	.18	.20	.21	.20	.15	.13	.16	.17	.22
$\Lambda\pi^+\pi^-\gamma^0$	.17	.21	.22	.27	.27	.29	.33	.37	.41
	.03	.04	.04	.04	.03	.03	.04	.04	.04
$\Sigma^0\gamma^+\gamma^-$	.59	.48	.63	.52	.54	.56	.54	.62	.53
	.06	.06	.07	.05	.04	.04	.05	.05	.05
$\Sigma^0\pi^+\pi^-\gamma^0$	.005	.04	.04	.12	.12	.16	.16	.17	.18
	.005	.02	.02	.02	.02	.02	.02	.03	.03
$\Sigma^+\pi^-$	1.94	1.86	1.74	1.64	1.70	1.65	1.64	1.75	1.95
	.11	.12	.12	.10	.08	.08	.08	.08	.11
$\Sigma^-\gamma^+$	1.56	1.33	1.38	1.46	1.15	1.20	1.20	1.34	1.53
	.09	.09	.09	.09	.06	.06	.06	.06	.09
$\Sigma^+\pi^-\pi^0$	.65	.70	.77	.70	.79	.77	.79	.90	1.04
	.06	.07	.08	.06	.05	.05	.06	.06	.08
$\Sigma^-\pi^+\pi^0$	.70	.78	.75	.82	.75	.76	.82	.86	.90
	.07	.08	.08	.07	.06	.05	.07	.07	.08
$\Sigma^+\pi^+\pi^-\gamma^-$	.007	.013	.003	.015	.026	.017	.034	.026	.051
	.005	.009	.003	.009	.008	.006	.010	.008	.014
$\Sigma^-\pi^+\pi^+\pi^-$	0.	0.	.004	.003	.005	.007	.010	.022	.013
			.004	.003	.004	.004	.005	.007	.008

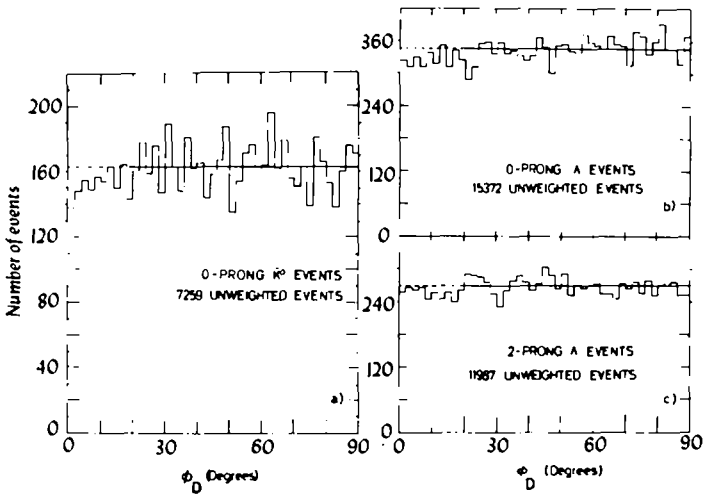

Fig. 2. (a) Distribution of the orientation of the K_S^0 decay plane with respect to the normal to the front window of the bubble chamber, as expressed by the azimuthal decay angle ϕ_D. (b, c) Same as 2(a) for 0-prong and 2-prong Λ events respectively.

5. Reactions involving a neutral decay

Special precautions have been taken in the analysis of 0-prong V^0 and 2-prong V^0 events, where the V^0 is either a $K_S^0 \to \pi^+\pi^-$ or a $\Lambda \to p\pi^-$. These follow closely the approach of previous experiments [1,9].

(a) To correct for the loss of V^0's decaying outside the fiducial volume or too close to the interaction vertex to be detected as a neutral decay, a weight is assigned to each event

$$W = \left[\exp\left(-\frac{l_0}{\lambda \cos\delta}\right) - \exp\left(-\frac{l_p}{\lambda}\right)\right]^{-1}. \tag{5.1}$$

Here $\lambda = \beta\gamma c\tau$ is the mean decay length of the V^0, δ the dip angle, l_p the potential decay length, and l_0 a cut-off projected length below which events have been rejected. The adopted values for l_0, beyond which there was no evidence of loss, were 2 mm for all 2-prong V^0 events, 3 mm for 0-prong Λ and 4 mm for 0-prong $\bar{K}^0$ events.

(b) Some V^0 decays may escape detection when their decay plane is normal to the front window of the chamber. The relevance of this bias may be checked by examining the distribution of the azimuthal decay angle ϕ_D defined by

$$\cos\phi_D = \frac{(\hat{Z}\times\hat{N})}{|\hat{Z}\times\hat{N}|}\cdot\frac{(\hat{N}\times\hat{d})}{|\hat{N}\times\hat{d}|}, \qquad 0^\circ \leqslant \phi_D \leqslant 90^\circ, \tag{5.2}$$

which should be isotropic in absence of losses. Here $\hat{Z}$ is the unit vector normal to

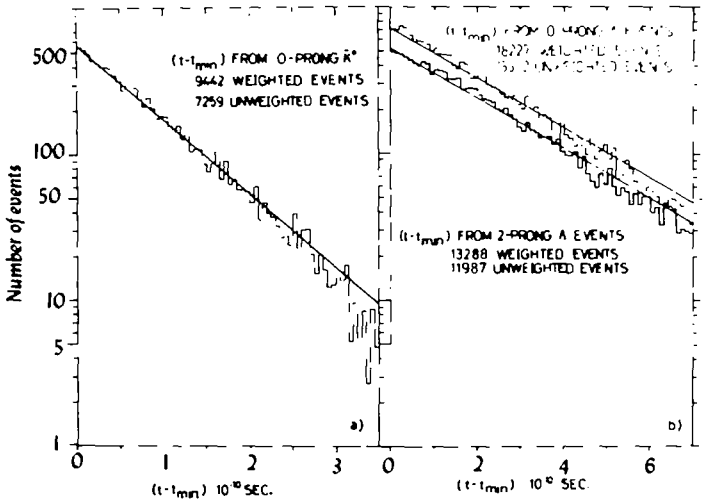

Fig. 3. (a) Distribution of the K_S^O lifetimes for 0-prong $\bar{K}^O$ events. $t_{min} = l_O/\beta\gamma c$ is the minimum observable lifetime (which depends on the K_S^O momentum) corresponding to our cut-off in K_S^O path length. The full line corresponds to a mean life of 0.862×10^{-10} sec[7]. (b) Same as 3(a) for Λ lifetimes from 0-prong Λ and 2-prong Λ events respectively. The full lines correspond to $\tau = 2.521 \times 10^{-10}$ sec [7].

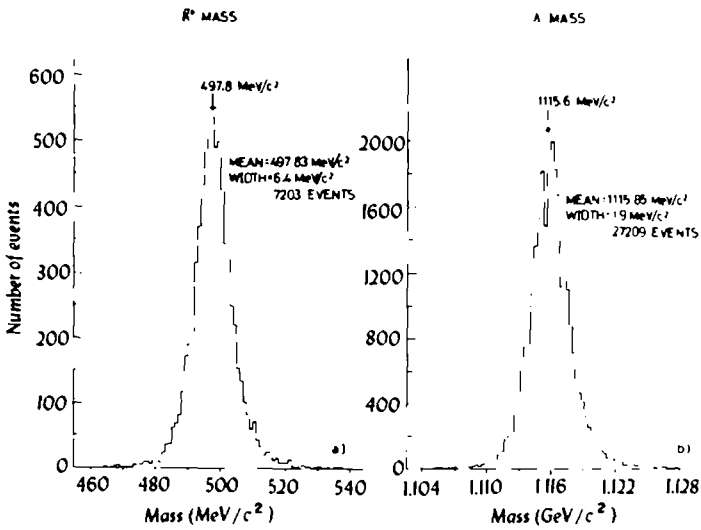

Fig. 4. (a) Distribution of the fitted values for the $\bar{K}^O$ mass, from 0-prong $\bar{K}^O$ events. Central value and standard deviation are indicated in the figure. (b) Distribution of the fitted values of the Λ mass from all Λ events. Central value and standard deviation are indicated in the figure.

the front window, $\hat{N}$ that along the flight path of the decay (neutral) particle, and $\hat{d}$ refers to one of the decay products. As shown in fig. 2, a loss of $\sim 1\%$ of the events near $\phi_D = 0^\circ$ can be detected for the 0-prong $\bar{K}^0$ events and is practically absent in 0-prong Λ and 2-prong Λ events. In view of the small size of the effect, no correction was introduced.

(c) Kinematical constraints usually suffice to distinguish Λ from $\bar{K}^0$ production at these energies. Those events which were kinematically ambiguous were distinguished by ionization, leaving only 12 out of 22 000 events as truly ambiguous.

(d) Following refs. [1,9], a further correction has been introduced for Λ decays, to account for the loss of decays at low momentum, in which the decay proton is emitted backwards in the c.m.s. This was introduced as a weight for each Λ event

$$W = \frac{2}{(1 - \cos\theta)}\ , \tag{5.3}$$

where θ, which depends on Λ momentum, is the decay angle in the Λ rest frame corresponding to a cut-off in proton lab momentum of 110 MeV/c.

As a result of the corrections described in (a) and (d), the average event weights were 1.11 for 2-prong Λ, 1.19 for 0-prong Λ, and 1.30 for 0-prong $\bar{K}^0$ events. Distributions of the K_S^0 lifetimes are shown in fig. 3(a); and of the Λ lifetimes, from 0-prong Λ and 2-prong Λ events separately, in fig. 3(b). For comparison, the decay lines corresponding to the accepted K_S^0 and Λ mean-lives [7] are also indicated. The $\bar{K}^0$ and Λ mass distributions, determined from 2-constraint fits to the decays, are shown in figs. 4(a) and 4(b) respectively. As indicated, excellent agreement is found between the measured masses and the standard values of ref. [7]. Fig. 4 also indicates the mass resolution attained in this experiment.

5.1. $\bar{K}^0$ reactions

In our momentum region, the following reactions contribute:

$$K^- p \to \bar{K}^0 n\ , \tag{5.4}$$

$$\to \bar{K}^0 n\pi^0\ , \tag{5.5}$$

$$\to \bar{K}^0 p\pi^-\ . \tag{5.6}$$

Only the fraction involving the decay $K_S^0 \to \pi^+\pi^-$ was studied. The separation between reactions (5.4) and (5.5) is unambiguous as illustrated in the MM^2 (missing mass squared) plot of fig. 5. In calculating cross sections, the branching ratio for $\bar{K}^0 \to \pi^+\pi^-$ was taken as 0.3442 [7]. The differential cross sections for reaction (5.4) are listed in table 4 and plotted in fig. 12. The corresponding Legendre polynomial coefficients appear in table 6. As usual, the latter refer to the expansion

$$d\sigma/d\Omega = \lambda^2 \sum_n A_n P_n(\cos\theta)\ . \tag{5.7}$$

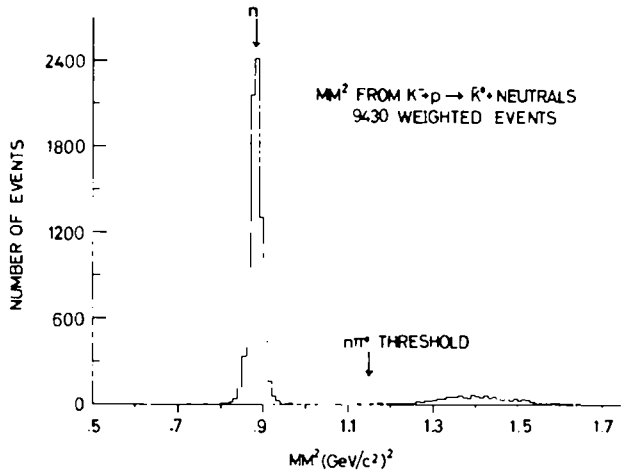

Fig. 5. Plot of the missing mass squared to the $\bar{K}^0$ for the reactions $K^-p \to \bar{K}^0$ + neutrals, indicating the separation between $\bar{K}^0n$ and $\bar{K}^0n\pi^0$ events.

These have been determined by a least-squares fit through A_6, with the chi-squared probability listed in table 6 along with the 0° and 180° cross sections obtained from the fit.

5.2. Λ *reactions*

The following reactions contribute:

$$K^-p \to \Lambda\pi^0 , \tag{5.8}$$

$$\to \Sigma^0\pi^0 , \tag{5.9}$$

$$\to \Lambda\pi^0\pi^0 , \tag{5.10}$$

$$\to \Sigma^0\pi^0\pi^0 , \tag{5.11}$$

$$\to \Lambda\pi^0\pi^0\pi^0 , \tag{5.12}$$

$$\to \Sigma^0\pi^0\pi^0\pi^0 , \tag{5.13}$$

$$\to \Lambda\pi^+\pi^- , \tag{5.14}$$

$$\to \Sigma^0\pi^+\pi^- , \tag{5.15}$$

$$\to \Lambda\pi^+\pi^-\pi^0 , \tag{5.16}$$

$$\to \Sigma^0\pi^+\pi^-\pi^0 , \tag{5.17}$$

$$\to \Lambda\eta , \tag{5.18}$$

$$\to \Sigma^0\eta . \tag{5.19}$$

Table 4
Differential cross sections

P_{K^-} = 862 MeV/c

$\bar{K}^0 n$ cos θ	dσ/dΩ (mb/ster)	ERROR	$\Lambda\pi^0$ cos θ	dσ/dΩ (mb/ster)	ERROR	$\Sigma^+\pi^-$ cos θ	dσ/dΩ (mb/ster)	ERROR	$\Sigma^-\pi^+$ cos θ	dσ/dΩ (mb/ster)	ERROR
-0.975	1.594	0.246	-0.975	0.872	0.113	-0.975	0.211	0.053	-0.975	0.226	0.048
-0.925	1.387	0.228	-0.925	0.605	0.095	-0.925	0.157	0.042	-0.925	0.275	0.053
-0.875	1.015	0.155	-0.875	0.534	0.089	-0.875	0.112	0.040	-0.875	0.241	0.050
-0.825	1.005	0.197	-0.825	0.463	0.083	-0.825	0.117	0.039	-0.825	0.225	0.048
-0.775	0.431	0.130	-0.775	0.665	0.101	-0.775	0.131	0.044	-0.775	0.236	0.049
-0.725	0.399	0.133	-0.725	0.422	0.077	-0.725	0.121	0.038	-0.725	0.156	0.040
-0.650	0.106	0.044	-0.675	0.575	0.092	-0.675	0.092	0.032	-0.675	0.253	0.052
-0.550	0.124	0.047	-0.625	0.278	0.062	-0.625	0.212	0.055	-0.625	0.197	0.045
-0.425	0.100	0.035	-0.575	0.381	0.075	-0.575	0.143	0.043	-0.575	0.112	0.034
-0.300	0.131	0.046	-0.525	0.318	0.069	-0.525	0.119	0.040	-0.525	0.148	0.040
-0.225	0.252	0.097	-0.475	0.300	0.066	-0.475	0.121	0.040	-0.475	0.101	0.032
-0.175	0.348	0.105	-0.425	0.167	0.048	-0.425	0.076	0.031	-0.425	0.106	0.034
-0.125	0.297	0.094	-0.375	0.314	0.067	-0.350	0.038	0.016	-0.375	0.051	0.023
-0.050	0.179	0.052	-0.325	0.135	0.045	-0.275	0.126	0.042	-0.300	0.058	0.017
0.025	0.642	0.140	-0.275	0.171	0.052	-0.225	0.163	0.047	-0.200	0.046	0.016
0.075	0.265	0.088	-0.225	0.205	0.054	-0.150	0.060	0.020	-0.100	0.057	0.017
0.125	0.644	0.141	-0.175	0.152	0.046	-0.075	0.056	0.025	0.0	0.031	0.013
0.175	0.268	0.089	-0.125	0.111	0.042	-0.025	0.088	0.033	0.100	0.037	0.014
0.225	0.285	0.090	-0.075	0.109	0.038	0.025	0.065	0.029	0.175	0.055	0.032
0.275	0.355	0.103	-0.025	0.113	0.040	0.100	0.059	0.020	0.225	0.096	0.032
0.325	0.377	0.104	0.025	0.108	0.038	0.175	0.117	0.039	0.275	0.065	0.026
0.375	0.547	0.126	0.100	0.053	0.020	0.225	0.138	0.042	0.325	0.096	0.032
0.425	0.343	0.099	0.225	0.028	0.011	0.275	0.153	0.044	0.375	0.089	0.031
0.475	0.352	0.102	0.375	0.034	0.013	0.325	0.145	0.044	0.425	0.097	0.032
0.525	0.373	0.103	0.500	0.066	0.022	0.375	0.127	0.040	0.475	0.097	0.032
0.575	0.393	0.109	0.575	0.132	0.044	0.425	0.234	0.057	0.525	0.122	0.037
0.625	0.210	0.079	0.625	0.150	0.047	0.475	0.265	0.059	0.575	0.091	0.032
0.675	0.223	0.079	0.675	0.249	0.060	0.525	0.263	0.060	0.625	0.114	0.036
0.725	0.378	0.105	0.725	0.205	0.056	0.575	0.275	0.063	0.675	0.078	0.030
0.775	0.250	0.083	0.775	0.370	0.074	0.625	0.216	0.056	0.725	0.135	0.040
0.825	0.326	0.098	0.825	0.553	0.092	0.675	0.298	0.067	0.775	0.156	0.043
0.875	0.391	0.104	0.875	0.681	0.104	0.725	0.326	0.071	0.825	0.237	0.054
0.925	0.318	0.096	0.925	0.634	0.107	0.775	0.280	0.068	0.875	0.195	0.050
0.975	0.145	0.065	0.975	0.902	0.157	0.825	0.355	0.079	0.925	0.248	0.059
						0.875	0.326	0.079	0.975	0.167	0.050
						0.950	0.122	0.037			
464 Events			730 Events			435 Events			452 Events		

Table 4 (continued)

P_{K^-} = 883 MeV/c

$\bar{K}^0 n$			$\Lambda\pi^0$			$\Sigma^+\pi^-$			$\Sigma^-\pi^+$		
cos θ	dσ/dΩ (mb/ster)	ERROR	cos θ	dσ/dΩ (mb/ster)	ERROR	cos θ	dσ/dΩ (mb/ster)	ERROR	cos θ	dσ/dΩ (mb/ster)	ERROR
-0.975	2.101	0.313	-0.975	0.717	0.112	-0.975	0.133	0.047	-0.975	0.162	0.045
-0.925	1.160	0.232	-0.925	0.735	0.112	-0.925	0.195	0.060	-0.925	0.231	0.053
-0.875	0.972	0.212	-0.875	0.652	0.106	-0.875	0.097	0.040	-0.875	0.182	0.047
-0.825	0.686	0.183	-0.825	0.621	0.108	-0.825	0.222	0.061	-0.825	0.166	0.044
-0.775	0.462	0.139	-0.775	0.451	0.087	-0.775	0.092	0.035	-0.775	0.215	0.051
-0.725	0.319	0.121	-0.725	0.485	0.092	-0.725	0.082	0.037	-0.725	0.101	0.036
-0.650	0.196	0.091	-0.675	0.292	0.073	-0.675	0.145	0.051	-0.675	0.272	0.058
-0.550	0.136	0.052	-0.625	0.353	0.077	-0.625	0.171	0.054	-0.625	0.082	0.031
-0.450	0.120	0.049	-0.575	0.315	0.072	-0.575	0.072	0.032	-0.575	0.188	0.047
-0.350	0.156	0.055	-0.525	0.181	0.055	-0.500	0.084	0.027	-0.525	0.121	0.038
-0.250	0.105	0.047	-0.475	0.304	0.076	-0.400	0.063	0.023	-0.475	0.087	0.033
-0.175	0.224	0.092	-0.425	0.283	0.071	-0.300	0.090	0.027	-0.425	0.125	0.040
-0.125	0.183	0.082	-0.375	0.148	0.049	-0.200	0.063	0.022	-0.325	0.036	0.012
-0.075	0.420	0.127	-0.325	0.186	0.059	-0.100	0.062	0.022	-0.175	0.032	0.011
-0.025	0.186	0.083	-0.275	0.166	0.053	0.0	0.038	0.017	-0.050	0.042	0.016
0.025	0.478	0.133	-0.225	0.143	0.051	0.075	0.090	0.037	0.050	0.036	0.015
0.075	0.435	0.126	-0.175	0.183	0.055	0.125	0.107	0.040	0.150	0.037	0.015
0.125	0.330	0.110	-0.125	0.085	0.038	0.175	0.110	0.042	0.225	0.111	0.037
0.175	0.282	0.100	-0.075	0.277	0.069	0.225	0.144	0.048	0.275	0.089	0.033
0.225	0.218	0.089	-0.025	0.100	0.041	0.300	0.092	0.026	0.325	0.117	0.039
0.275	0.433	0.125	0.025	0.135	0.048	0.375	0.241	0.062	0.375	0.115	0.038
0.325	0.283	0.100	0.075	0.136	0.048	0.425	0.114	0.043	0.425	0.102	0.036
0.375	0.386	0.116	0.175	0.039	0.015	0.475	0.242	0.063	0.475	0.069	0.028
0.425	0.498	0.133	0.300	0.060	0.023	0.525	0.182	0.055	0.525	0.141	0.042
0.475	0.500	0.134	0.400	0.052	0.021	0.575	0.283	0.069	0.575	0.117	0.039
0.525	0.280	0.099	0.500	0.049	0.020	0.625	0.246	0.066	0.625	0.078	0.032
0.575	0.436	0.126	0.575	0.137	0.048	0.675	0.242	0.065	0.675	0.144	0.044
0.625	0.218	0.089	0.625	0.151	0.050	0.725	0.278	0.072	0.750	0.075	0.023
0.675	0.341	0.108	0.675	0.225	0.062	0.775	0.372	0.085	0.825	0.160	0.048
0.725	0.394	0.119	0.725	0.457	0.090	0.825	0.378	0.089	0.875	0.133	0.044
0.775	0.285	0.101	0.775	0.407	0.085	0.875	0.299	0.083	0.925	0.241	0.062
0.825	0.416	0.120	0.825	0.376	0.082	0.950	0.190	0.051	0.975	0.119	0.045
0.875	0.242	0.091	0.875	0.657	0.111						
0.925	0.304	0.101	0.925	0.548	0.110						
0.975	0.214	0.087	0.975	0.496	0.124						
378 Events			602 Events			336 Events			332 Events		

Table 4 (continued)

P_{K^-} = 888 MeV/c

$\bar{K}^0 n$			$\Lambda\pi^0$			$\Sigma^+\pi^-$			$\Sigma^-\pi^+$		
cos θ	dσ/dΩ (mb/ster)	ERROR	cos θ	dσ/dΩ (mb/ster)	ERROR	cos θ	dσ/dΩ (mb/ster)	ERROR	cos θ	dσ/dΩ (mb/ster)	ERROR
-0.975	1.841	0.299	-0.975	0.983	0.136	-0.950	0.075	0.025	-0.975	0.225	0.055
-0.925	2.186	0.326	-0.925	0.84C	0.128	-0.875	0.155	0.055	-0.925	0.188	0.050
-0.875	1.15C	C.235	-0.875	0.754	0.122	-0.825	0.255	C.071	-0.875	0.242	0.057
-0.825	C.738	0.190	-0.825	C.476	0.097	-0.775	0.170	0.057	-0.825	0.264	0.059
-0.775	C.491	0.155	-0.775	C.538	0.102	-C.725	C.085	0.040	-0.775	0.262	C.060
-0.700	0.168	0.070	-0.725	0.538	0.104	-0.675	0.07C	0.031	-0.725	0.207	0.053
-0.575	0.073	0.033	-0.675	0.466	0.093	-0.600	0.069	0.025	-0.675	0.187	0.050
-0.450	C.1C7	C.048	-0.625	0.522	C.10C	-0.500	0.1C2	0.031	-0.625	C.171	C.048
-C.350	C.120	0.049	-0.575	0.191	0.060	-0.425	0.088	0.039	-0.575	0.071	0.022
-0.250	0.118	0.048	-0.525	0.217	0.063	-0.375	0.079	0.035	-0.525	C.13C	0.041
-0.175	0.188	0.084	-0.475	0.264	0.071	-0.275	0.026	0.012	-0.475	C.131	0.041
-0.125	0.243	C.C99	-0.425	0.255	0.071	-0.125	0.046	0.016	-0.400	0.052	0.018
-0.075	0.357	0.119	-0.375	0.2C5	0.062	0.0	0.048	0.020	-0.3C0	C.066	0.021
-0.025	0.3C3	0.107	-0.325	0.193	0.061	0.100	0.077	0.026	-0.200	0.033	0.015
0.025	0.317	0.112	-0.275	0.215	0.065	0.200	0.114	0.032	-0.075	0.027	0.011
0.075	0.342	0.114	-0.225	0.231	C.067	C.275	0.185	0.056	0.050	C.04C	0.017
0.125	0.649	0.151	-0.175	0.154	0.055	0.325	0.103	0.042	0.150	0.068	0.022
0.175	0.338	0.113	-0.125	0.147	0.052	0.375	0.141	0.050	0.225	C.081	0.033
0.225	0.3C2	0.107	-0.075	C.112	0.046	0.425	0.284	C.071	0.275	0.068	C.030
0.275	C.342	0.114	-0.025	0.150	0.053	0.475	0.282	0.071	0.325	0.082	0.033
0.325	0.492	0.136	0.025	0.054	0.042	0.525	0.122	0.045	0.375	C.C83	0.034
0.375	C.438	0.126	0.075	0.191	0.060	0.575	C.277	C.C72	0.425	0.07C	0.031
0.425	C.265	0.1CC	0.150	0.094	0.030	0.625	0.281	0.073	0.475	0.127	0.042
0.475	0.329	0.110	0.250	C.C86	0.029	0.675	0.181	0.060	0.525	0.114	C.04C
0.525	C.4CC	C.12C	0.375	0.032	0.014	0.725	0.292	0.075	0.575	0.085	0.035
0.575	0.479	0.133	C.5C0	0.046	C.021	0.775	0.241	0.070	0.625	0.072	0.032
0.625	0.282	C.106	0.575	C.058	C.044	0.825	0.37C	C.092	0.675	C.089	0.036
0.675	C.214	C.087	0.625	0.231	0.067	0.875	0.328	0.091	0.725	0.139	0.046
0.725	0.45C	0.130	0.675	C.291	0.075	0.950	C.180	0.054	0.800	0.056	0.021
0.775	C.411	0.124	0.725	0.412	0.090				0.875	0.132	0.047
0.825	0.30C	0.106	0.775	0.233	0.067				0.925	0.248	0.066
0.875	0.330	0.110	0.825	0.458	C.C96				0.975	C.228	0.066
0.950	C.210	0.063	0.875	0.849	0.133						
			0.925	0.773	0.135						
			975	C.728	0.163						
377 Events			613 Events			289 Events			312 Events		

Table 4 (continued)

P_{K^-} = 902 MeV/c

$\bar{K}^0 n$			$\pi^0 n$			$\Sigma^+\pi^-$			$\Sigma^-\pi^+$		
cos θ	dσ/dΩ (mb/ster)	ERROR	cos θ	dσ/dΩ (mb/ster)	ERROR	cos θ	dσ/dΩ (mb/ster)	ERROR	cos θ	dσ/dΩ (mb/ster)	ERROR
-0.975	1.962	0.272	-0.975	0.804	0.111	-0.975	0.172	0.052	-0.975	0.177	0.043
-0.925	1.000	0.192	-0.925	0.565	0.096	-0.925	0.240	0.062	-0.925	0.183	0.044
-0.875	1.327	0.224	-0.875	0.592	0.092	-0.875	0.073	0.030	-0.875	0.246	0.051
-0.825	0.587	0.157	-0.825	0.677	0.100	-0.825	0.144	0.043	-0.825	0.212	0.047
-0.775	0.502	0.139	-0.775	0.646	0.099	-0.775	0.099	0.038	-0.775	0.336	0.059
-0.725	0.471	0.136	-0.725	0.363	0.073	-0.725	0.158	0.048	-0.725	0.206	0.047
-0.650	0.198	0.067	-0.675	0.477	0.093	-0.675	0.068	0.030	-0.675	0.206	0.046
-0.550	0.132	0.047	-0.625	0.382	0.076	-0.625	0.136	0.043	-0.625	0.159	0.041
-0.450	0.100	0.041	-0.575	0.265	0.062	-0.575	0.148	0.047	-0.575	0.103	0.033
-0.375	0.200	0.082	-0.525	0.266	0.063	-0.525	0.100	0.035	-0.525	0.190	0.045
-0.325	0.164	0.073	-0.475	0.235	0.059	-0.450	0.042	0.017	-0.475	0.128	0.037
-0.275	0.165	0.074	-0.425	0.325	0.072	-0.350	0.072	0.023	-0.400	0.052	0.017
-0.225	0.227	0.086	-0.375	0.260	0.063	-0.250	0.035	0.016	-0.300	0.028	0.012
-0.175	0.246	0.087	-0.325	0.330	0.072	-0.150	0.042	0.016	-0.200	0.048	0.016
-0.125	0.337	0.102	-0.275	0.233	0.058	-0.050	0.036	0.016	-0.100	0.058	0.018
-0.075	0.334	0.101	-0.225	0.219	0.056	0.050	0.036	0.015	-0.025	0.095	0.032
-0.025	0.414	0.111	-0.175	0.227	0.055	0.125	0.124	0.039	0.025	0.065	0.027
0.025	0.389	0.108	-0.125	0.154	0.049	0.175	0.056	0.036	0.075	0.076	0.029
0.075	0.292	0.092	-0.075	0.186	0.054	0.225	0.152	0.044	0.125	0.086	0.030
0.125	0.529	0.125	-0.025	0.202	0.054	0.275	0.181	0.050	0.200	0.032	0.013
0.175	0.654	0.145	0.025	0.117	0.041	0.325	0.050	0.034	0.275	0.088	0.031
0.225	0.502	0.122	0.075	0.158	0.048	0.375	0.170	0.047	0.325	0.054	0.024
0.275	0.555	0.133	0.125	0.134	0.045	0.425	0.075	0.032	0.400	0.071	0.020
0.325	0.323	0.097	0.200	0.072	0.023	0.475	0.164	0.047	0.475	0.124	0.037
0.375	0.462	0.119	0.300	0.085	0.025	0.525	0.180	0.050	0.525	0.075	0.030
0.425	0.458	0.115	0.400	0.080	0.024	0.575	0.282	0.063	0.575	0.124	0.037
0.475	0.386	0.107	0.475	0.072	0.032	0.625	0.341	0.070	0.650	0.046	0.016
0.525	0.195	0.075	0.525	0.115	0.041	0.675	0.264	0.062	0.725	0.095	0.033
0.575	0.356	0.103	0.575	0.206	0.055	0.725	0.265	0.063	0.775	0.085	0.032
0.625	0.253	0.084	0.625	0.103	0.039	0.775	0.359	0.077	0.825	0.178	0.048
0.675	0.338	0.097	0.675	0.284	0.065	0.825	0.258	0.066	0.875	0.184	0.049
0.725	0.345	0.100	0.725	0.229	0.059	0.875	0.165	0.055	0.925	0.223	0.056
0.775	0.361	0.100	0.775	0.343	0.072	0.950	0.087	0.031	0.975	0.264	0.064
0.825	0.200	0.075	0.825	0.503	0.089						
0.875	0.309	0.093	0.875	0.702	0.106						
0.925	0.226	0.080	0.925	0.748	0.118						
0.975	0.224	0.079	0.975	0.792	0.145						
498 Events			791 Events			361 Events			413 Events		

Table 4 (continued)

P_{K^-} = 918 MeV/c

$\bar{K}^0 n$			π^0			$\pi^+\pi^-$			$\pi^-\pi^+$		
cos θ	dσ/dΩ (mb/ster)	ERROR	cos θ	dσ/dΩ (mb/ster)	ERROR	cos θ	dσ/dΩ (mb/ster)	ERROR	cos θ	dσ/dΩ (mb/ster)	ERROR
-0.975	1.492	0.191	-0.975	0.753	0.085	-0.975	0.086	0.029	-0.975	0.136	0.030
-0.925	1.531	0.193	-0.925	0.545	0.071	-0.925	0.145	0.036	-0.925	0.208	0.038
-0.875	0.975	0.156	-0.875	0.571	0.076	-0.875	0.109	0.033	-0.875	0.202	0.037
-0.825	0.750	0.135	-0.825	0.621	0.080	-0.825	0.110	0.032	-0.825	0.255	0.041
-0.775	0.423	0.097	-0.775	0.417	0.064	-0.775	0.099	0.033	-0.775	0.183	0.035
-0.725	0.377	0.101	-0.725	0.333	0.057	-0.725	0.104	0.033	-0.725	0.184	0.035
-0.650	0.076	0.031	-0.675	0.361	0.059	-0.675	0.112	0.032	-0.675	0.223	0.039
-0.550	0.078	0.032	-0.625	0.405	0.064	-0.625	0.110	0.030	-0.625	0.248	0.041
-0.450	0.054	0.024	-0.575	0.228	0.047	-0.575	0.079	0.025	-0.575	0.082	0.024
-0.375	0.153	0.058	-0.525	0.255	0.050	-0.500	0.053	0.015	-0.525	0.115	0.028
-0.325	0.245	0.072	-0.475	0.239	0.048	-0.425	0.048	0.021	-0.475	0.122	0.029
-0.275	0.165	0.058	-0.425	0.331	0.060	-0.375	0.043	0.019	-0.425	0.060	0.020
-0.225	0.127	0.052	-0.375	0.266	0.053	-0.325	0.035	0.018	-0.375	0.088	0.024
-0.175	0.154	0.054	-0.325	0.247	0.050	-0.225	0.013	0.006	-0.300	0.034	0.011
-0.125	0.311	0.080	-0.275	0.212	0.045	-0.125	0.071	0.025	-0.225	0.047	0.018
-0.075	0.262	0.073	-0.225	0.165	0.040	-0.075	0.049	0.020	-0.175	0.042	0.017
-0.025	0.356	0.084	-0.175	0.170	0.040	-0.025	0.040	0.018	-0.125	0.063	0.021
0.025	0.361	0.085	-0.125	0.213	0.045	0.025	0.045	0.020	-0.075	0.054	0.019
0.075	0.289	0.075	-0.075	0.196	0.044	0.075	0.076	0.025	-0.025	0.047	0.018
0.125	0.430	0.092	-0.025	0.215	0.045	0.125	0.088	0.027	0.050	0.034	0.011
0.175	0.509	0.100	0.025	0.165	0.040	0.175	0.126	0.033	0.125	0.062	0.021
0.225	0.441	0.092	0.075	0.114	0.033	0.225	0.147	0.035	0.175	0.034	0.015
0.275	0.416	0.089	0.125	0.152	0.038	0.275	0.175	0.038	0.225	0.048	0.018
0.325	0.506	0.097	0.175	0.118	0.034	0.325	0.168	0.037	0.275	0.091	0.025
0.375	0.299	0.075	0.225	0.132	0.035	0.375	0.178	0.039	0.325	0.057	0.020
0.425	0.300	0.075	0.275	0.157	0.039	0.425	0.174	0.039	0.400	0.026	0.010
0.475	0.300	0.075	0.325	0.085	0.030	0.475	0.228	0.045	0.500	0.025	0.010
0.525	0.349	0.080	0.375	0.073	0.026	0.525	0.222	0.044	0.575	0.036	0.016
0.575	0.365	0.084	0.425	0.103	0.031	0.575	0.336	0.055	0.625	0.036	0.016
0.625	0.188	0.060	0.475	0.078	0.028	0.625	0.251	0.048	0.675	0.051	0.019
0.675	0.356	0.082	0.525	0.137	0.037	0.675	0.261	0.050	0.725	0.052	0.020
0.725	0.224	0.065	0.575	0.137	0.037	0.725	0.382	0.061	0.775	0.054	0.020
0.775	0.259	0.069	0.625	0.134	0.036	0.775	0.274	0.053	0.825	0.085	0.027
0.825	0.317	0.077	0.675	0.256	0.050	0.825	0.344	0.062	0.875	0.115	0.031
0.875	0.448	0.093	0.725	0.265	0.051	0.875	0.175	0.045	0.925	0.150	0.037
0.925	0.256	0.068	0.775	0.288	0.054	0.925	0.240	0.058	0.975	0.185	0.042
0.975	0.147	0.052	0.825	0.445	0.067	0.975	0.115	0.043			
			0.875	0.583	0.077						
			0.925	0.746	0.093						
			0.975	0.728	0.110						
687 Events			1142 Events			576 Events			516 Events		

Table 4 (continued)

P_{K^-} = 971 MeV/c

$\bar{K}^0 n$			$\Lambda\pi^0$			$\Sigma^+\pi^-$			$\Sigma^-\pi^+$		
cos θ	dσ/dΩ (mb/ster)	ERROR	cos θ	dσ/dΩ (mb/ster)	ERROR	cos θ	dσ/dΩ (mb/ster)	ERROR	cos θ	dσ/dΩ (mb/ster)	ERROR
-0.975	1.895	0.212	-0.975	0.670	0.081	-0.975	0.181	0.039	-0.975	0.178	0.034
-0.925	1.683	0.198	-0.925	0.612	0.079	-0.925	0.126	0.034	-0.925	0.189	0.036
-0.875	1.349	0.180	-0.875	0.418	0.064	-0.875	0.152	0.036	-0.875	0.248	0.040
-0.825	0.718	0.131	-0.825	0.573	0.075	-0.825	0.124	0.032	-0.825	0.205	0.037
-0.775	0.546	0.109	-0.775	0.385	0.062	-0.775	0.077	0.027	-0.775	0.240	0.040
-0.725	0.534	0.111	-0.725	0.301	0.053	-0.725	0.136	0.035	-0.725	0.235	0.039
-0.675	0.188	0.071	-0.675	0.387	0.063	-0.675	0.081	0.027	-0.675	0.272	0.042
-0.600	0.076	0.029	-0.625	0.345	0.057	-0.625	0.076	0.025	-0.625	0.179	0.034
-0.525	0.100	0.045	-0.575	0.267	0.051	-0.575	0.097	0.029	-0.575	0.199	0.036
-0.475	0.097	0.043	-0.525	0.354	0.057	-0.525	0.075	0.026	-0.525	0.171	0.034
-0.425	0.237	0.071	-0.475	0.277	0.051	-0.475	0.056	0.021	-0.475	0.161	0.033
-0.375	0.125	0.051	-0.425	0.340	0.058	-0.425	0.053	0.022	-0.425	0.170	0.033
-0.325	0.243	0.070	-0.375	0.253	0.049	-0.375	0.038	0.017	-0.375	0.106	0.027
-0.275	0.414	0.090	-0.325	0.245	0.048	-0.275	0.014	0.006	-0.325	0.124	0.028
-0.225	0.181	0.060	-0.275	0.309	0.052	-0.150	0.040	0.013	-0.275	0.052	0.019
-0.175	0.548	0.104	-0.225	0.200	0.044	-0.050	0.038	0.012	-0.225	0.075	0.022
-0.125	0.609	0.109	-0.175	0.213	0.044	0.025	0.055	0.021	-0.150	0.043	0.012
-0.075	0.442	0.092	-0.125	0.205	0.045	0.075	0.076	0.024	-0.075	0.035	0.016
-0.025	0.606	0.109	-0.075	0.181	0.042	0.125	0.132	0.032	-0.025	0.083	0.024
0.025	0.707	0.116	-0.025	0.123	0.034	0.175	0.160	0.036	0.025	0.034	0.015
0.075	0.492	0.097	0.025	0.181	0.041	0.225	0.121	0.030	0.075	0.082	0.024
0.125	0.654	0.111	0.075	0.141	0.036	0.275	0.179	0.038	0.125	0.088	0.024
0.175	0.460	0.094	0.125	0.279	0.051	0.325	0.253	0.045	0.175	0.068	0.021
0.225	0.425	0.089	0.175	0.245	0.047	0.375	0.191	0.040	0.225	0.095	0.026
0.275	0.469	0.094	0.225	0.112	0.032	0.425	0.352	0.054	0.275	0.056	0.020
0.325	0.596	0.105	0.275	0.228	0.047	0.475	0.142	0.035	0.325	0.081	0.023
0.375	0.570	0.104	0.325	0.225	0.046	0.525	0.333	0.053	0.375	0.034	0.015
0.425	0.375	0.084	0.375	0.120	0.033	0.575	0.310	0.052	0.425	0.055	0.020
0.475	0.509	0.096	0.425	0.188	0.042	0.625	0.365	0.057	0.500	0.027	0.010
0.525	0.549	0.100	0.475	0.176	0.040	0.675	0.301	0.052	0.600	0.021	0.009
0.575	0.469	0.092	0.525	0.291	0.052	0.725	0.249	0.048	0.700	0.043	0.012
0.625	0.320	0.076	0.575	0.242	0.047	0.775	0.321	0.055	0.800	0.034	0.012
0.675	0.344	0.079	0.625	0.207	0.044	0.825	0.210	0.047	0.875	0.122	0.032
0.725	0.455	0.091	0.675	0.217	0.045	0.875	0.217	0.050	0.925	0.118	0.032
0.775	0.469	0.094	0.725	0.390	0.061	0.950	0.065	0.021	0.975	0.179	0.041
0.825	0.603	0.103	0.775	0.353	0.058						
0.875	0.555	0.103	0.825	0.305	0.055						
0.925	0.559	0.102	0.875	0.469	0.068						
0.975	0.610	0.106	0.925	0.568	0.079						
			0.975	0.726	0.109						
1036 Events			1247 Events			639 Events			623 Events		

Table 4 (continued)

P_{K^-} = 1001 MeV/c

$\bar{K}^0 n$			π^0			$\pi^+\pi^-$			$\pi^-\pi^+$		
cos θ	dσ/dΩ (mb/ster)	ERROR	cos θ	dσ/dΩ (mb/ster)	ERROR	cos θ	dσ/dΩ (mb/ster)	ERROR	cos θ	dσ/dΩ (mb/ster)	ERROR
-0.975	2.658	0.303	-0.975	0.395	0.073	-0.975	0.215	0.057	-0.975	0.048	0.021
-0.925	2.015	0.262	-0.925	0.418	0.075	-0.925	0.129	0.039	-0.925	0.135	0.036
-0.875	1.180	0.199	-0.875	0.562	0.090	-0.875	0.145	0.046	-0.875	0.309	0.055
-0.825	1.192	0.202	-0.825	0.372	0.069	-0.825	0.230	0.053	-0.825	0.324	0.057
-0.775	0.690	0.151	-0.775	0.423	0.076	-0.775	0.172	0.050	-0.775	0.280	0.052
-0.725	0.334	0.101	-0.725	0.364	0.073	-0.700	0.063	0.020	-0.725	0.393	0.063
-0.675	0.364	0.110	-0.675	0.356	0.071	-0.625	0.086	0.032	-0.675	0.266	0.052
-0.600	0.181	0.061	-0.625	0.273	0.061	-0.575	0.095	0.034	-0.625	0.357	0.059
-0.525	0.209	0.079	-0.575	0.348	0.070	-0.525	0.057	0.025	-0.575	0.164	0.040
-0.475	0.151	0.067	-0.525	0.233	0.056	-0.475	0.083	0.031	-0.525	0.202	0.045
-0.425	0.266	0.089	-0.475	0.301	0.067	-0.350	0.020	0.008	-0.475	0.217	0.046
-0.375	0.241	0.085	-0.425	0.269	0.060	-0.150	0.014	0.006	-0.425	0.143	0.037
-0.325	0.357	0.103	-0.375	0.264	0.061	0.0	0.061	0.019	-0.375	0.077	0.027
-0.275	0.411	0.110	-0.325	0.151	0.045	0.075	0.058	0.026	-0.325	0.081	0.029
-0.225	0.443	0.111	-0.275	0.210	0.053	0.125	0.117	0.037	-0.275	0.068	0.026
-0.175	0.428	0.113	-0.225	0.230	0.058	0.175	0.109	0.036	-0.225	0.078	0.028
-0.125	0.618	0.132	-0.175	0.207	0.053	0.225	0.157	0.044	-0.175	0.067	0.025
-0.075	0.470	0.114	-0.125	0.223	0.054	0.275	0.137	0.040	-0.125	0.068	0.026
-0.025	0.416	0.107	-0.075	0.169	0.047	0.325	0.341	0.069	-0.075	0.080	0.028
0.025	0.422	0.109	-0.025	0.287	0.061	0.375	0.311	0.062	-0.025	0.050	0.022
0.075	0.604	0.129	0.025	0.160	0.046	0.425	0.280	0.058	0.025	0.080	0.028
0.125	0.549	0.123	0.075	0.079	0.032	0.475	0.324	0.064	0.075	0.089	0.030
0.175	0.498	0.117	0.125	0.170	0.047	0.525	0.407	0.072	0.125	0.108	0.033
0.225	0.495	0.117	0.175	0.130	0.041	0.575	0.233	0.053	0.175	0.059	0.024
0.275	0.548	0.123	0.225	0.166	0.048	0.625	0.381	0.071	0.225	0.065	0.026
0.325	0.811	0.148	0.275	0.207	0.053	0.675	0.375	0.071	0.300	0.050	0.016
0.375	0.376	0.101	0.325	0.225	0.055	0.725	0.301	0.064	0.375	0.061	0.025
0.425	0.278	0.088	0.375	0.157	0.045	0.775	0.257	0.061	0.425	0.052	0.021
0.475	0.385	0.103	0.425	0.190	0.049	0.825	0.257	0.062	0.500	0.047	0.016
0.525	0.523	0.120	0.475	0.235	0.057	0.875	0.127	0.045	0.625	0.018	0.008
0.575	0.446	0.108	0.525	0.137	0.043	0.925	0.297	0.074	0.750	0.055	0.017
0.625	0.600	0.128	0.575	0.287	0.061	0.975	0.141	0.053	0.850	0.076	0.021
0.675	0.603	0.126	0.625	0.272	0.061				0.925	0.187	0.048
0.725	0.320	0.092	0.675	0.175	0.050				0.975	0.204	0.053
0.775	0.864	0.156	0.725	0.335	0.067						
0.825	0.800	0.146	0.775	0.404	0.074						
0.875	0.922	0.156	0.825	0.335	0.068						
0.925	1.184	0.179	0.875	0.364	0.071						
0.975	0.901	0.152	0.925	0.380	0.076						
			0.975	0.357	0.087						
848 Events			782 Events			472 Events			478 Events		

Table 4 (continued)

P_{K^-} = 936 MeV/c

$\bar{K}^0 n$			Λ^0			$\Sigma^+\pi^-$			$\Sigma^-\pi^+$		
cos θ	dσ/dΩ (mb/ster)	ERROR	cos θ	dσ/dΩ (mb/ster)	ERROR	cos θ	dσ/dΩ (mb/ster)	ERROR	cos θ	dσ/dΩ (mb/ster)	ERROR
-0.975	1.677	0.182	-0.975	0.624	0.070	-0.975	0.189	0.037	-0.975	0.093	0.022
-0.925	1.280	0.159	-0.925	0.606	0.069	-0.925	0.123	0.028	-0.925	0.188	0.033
-0.875	1.201	0.153	-0.875	0.402	0.055	-0.875	0.143	0.034	-0.875	0.185	0.032
-0.825	1.025	0.143	-0.825	0.497	0.062	-0.825	0.072	0.021	-0.825	0.265	0.039
-0.775	0.584	0.112	-0.775	0.460	0.060	-0.775	0.128	0.031	-0.775	0.219	0.035
-0.725	0.300	0.078	-0.725	0.350	0.056	-0.725	0.136	0.032	-0.725	0.287	0.040
-0.675	0.135	0.055	-0.675	0.471	0.061	-0.675	0.069	0.022	-0.675	0.203	0.033
-0.625	0.170	0.060	-0.625	0.385	0.056	-0.625	0.074	0.022	-0.625	0.177	0.032
-0.575	0.168	0.056	-0.575	0.351	0.054	-0.575	0.061	0.021	-0.575	0.224	0.035
-0.525	0.098	0.044	-0.525	0.328	0.050	-0.525	0.074	0.022	-0.525	0.107	0.024
-0.475	0.088	0.039	-0.475	0.292	0.049	-0.475	0.050	0.019	-0.475	0.147	0.028
-0.425	0.161	0.054	-0.425	0.175	0.037	-0.425	0.039	0.017	-0.425	0.105	0.024
-0.375	0.113	0.043	-0.375	0.290	0.048	-0.375	0.039	0.017	-0.375	0.055	0.017
-0.325	0.170	0.054	-0.325	0.238	0.043	-0.300	0.030	0.011	-0.325	0.082	0.021
-0.275	0.236	0.063	-0.275	0.138	0.032	-0.200	0.040	0.012	-0.275	0.054	0.017
-0.225	0.276	0.067	-0.225	0.188	0.038	-0.100	0.032	0.011	-0.225	0.067	0.019
-0.175	0.247	0.064	-0.175	0.283	0.047	-0.025	0.046	0.019	-0.175	0.067	0.019
-0.125	0.406	0.083	-0.125	0.210	0.042	0.025	0.065	0.021	-0.125	0.044	0.015
-0.075	0.512	0.090	-0.075	0.096	0.027	0.075	0.045	0.017	-0.075	0.051	0.017
-0.025	0.553	0.093	-0.025	0.170	0.036	0.125	0.095	0.025	-0.025	0.055	0.017
0.025	0.348	0.074	0.025	0.163	0.036	0.175	0.118	0.029	0.025	0.045	0.016
0.075	0.494	0.089	0.075	0.149	0.034	0.225	0.131	0.030	0.075	0.034	0.014
0.125	0.437	0.083	0.125	0.228	0.042	0.275	0.198	0.037	0.125	0.067	0.019
0.175	0.557	0.093	0.175	0.141	0.032	0.325	0.122	0.029	0.175	0.045	0.016
0.225	0.486	0.087	0.225	0.068	0.023	0.375	0.130	0.031	0.225	0.034	0.014
0.275	0.405	0.079	0.275	0.113	0.029	0.425	0.211	0.039	0.275	0.051	0.017
0.325	0.464	0.085	0.325	0.169	0.036	0.475	0.241	0.042	0.325	0.046	0.016
0.375	0.373	0.076	0.375	0.121	0.030	0.525	0.208	0.039	0.375	0.033	0.014
0.425	0.312	0.070	0.425	0.173	0.036	0.575	0.324	0.049	0.425	0.069	0.020
0.475	0.375	0.077	0.475	0.114	0.030	0.625	0.344	0.051	0.475	0.071	0.020
0.525	0.345	0.072	0.525	0.130	0.031	0.675	0.316	0.049	0.550	0.027	0.009
0.575	0.289	0.066	0.575	0.146	0.034	0.725	0.270	0.046	0.625	0.030	0.013
0.625	0.378	0.076	0.625	0.257	0.045	0.775	0.255	0.046	0.675	0.030	0.014
0.675	0.441	0.082	0.675	0.232	0.042	0.825	0.226	0.045	0.725	0.037	0.015
0.725	0.345	0.072	0.725	0.313	0.050	0.875	0.211	0.045	0.800	0.044	0.012
0.775	0.337	0.072	0.775	0.370	0.054	0.925	0.147	0.041	0.875	0.095	0.025
0.825	0.330	0.070	0.825	0.453	0.060	0.975	0.138	0.044	0.925	0.151	0.033
0.875	0.253	0.063	0.875	0.485	0.063				0.975	0.156	0.035
0.925	0.262	0.063	0.925	0.558	0.072						
0.975	0.239	0.060	0.975	0.480	0.081						
985 Events			1427 Events			691 Events			662 Events		

Table 4 (continued)

p_{K^-} = 960 MeV/c

$\bar{K}^0 n$			π^0			$\pi^+\pi^-$			$\pi^-\pi^+$		
cos θ	dσ/dΩ (mb/ster)	ERROR	cos θ	dσ/dΩ (mb/ster)	ERROR	cos θ	dσ/dΩ (mb/ster)	ERROR	cos θ	dσ/dΩ (mb/ster)	ERROR
-0.975	1.878	0.221	-0.975	0.512	0.072	-0.975	0.110	0.035	-0.975	0.137	0.032
-0.925	1.731	0.211	-0.925	0.401	0.064	-0.925	0.105	0.034	-0.925	0.183	0.037
-0.875	1.289	0.186	-0.875	0.540	0.078	-0.875	0.194	0.045	-0.875	0.189	0.037
-0.825	0.747	0.139	-0.825	0.478	0.069	-0.825	0.050	0.032	-0.825	0.239	0.041
-0.775	0.450	0.103	-0.775	0.585	0.078	-0.775	0.085	0.027	-0.775	0.216	0.039
-0.725	0.329	0.088	-0.725	0.384	0.064	-0.725	0.051	0.019	-0.725	0.267	0.043
-0.675	0.237	0.075	-0.675	0.259	0.053	-0.675	0.119	0.032	-0.675	0.218	0.040
-0.625	0.252	0.084	-0.625	0.405	0.064	-0.625	0.078	0.026	-0.625	0.207	0.038
-0.550	0.077	0.029	-0.575	0.334	0.059	-0.575	0.060	0.025	-0.575	0.175	0.035
-0.475	0.136	0.056	-0.525	0.284	0.055	-0.500	0.024	0.011	-0.525	0.146	0.032
-0.425	0.156	0.059	-0.475	0.223	0.049	-0.375	0.023	0.008	-0.475	0.085	0.024
-0.375	0.165	0.062	-0.425	0.218	0.048	-0.225	0.016	0.007	-0.425	0.099	0.026
-0.325	0.112	0.050	-0.375	0.236	0.048	-0.100	0.023	0.009	-0.375	0.078	0.023
-0.275	0.150	0.057	-0.325	0.247	0.050	-0.025	0.061	0.025	-0.325	0.085	0.025
-0.225	0.244	0.074	-0.275	0.284	0.054	0.025	0.081	0.027	-0.275	0.069	0.022
-0.175	0.411	0.094	-0.225	0.253	0.052	0.075	0.069	0.024	-0.225	0.104	0.027
-0.125	0.318	0.082	-0.175	0.145	0.039	0.125	0.092	0.028	-0.150	0.032	0.010
-0.075	0.487	0.107	-0.125	0.163	0.041	0.175	0.064	0.030	-0.075	0.056	0.020
-0.025	0.483	0.101	-0.075	0.172	0.042	0.225	0.117	0.032	-0.025	0.071	0.023
0.025	0.532	0.105	-0.025	0.149	0.038	0.275	0.196	0.042	0.050	0.035	0.011
0.075	0.560	0.108	0.025	0.216	0.047	0.325	0.146	0.036	0.150	0.040	0.012
0.125	0.562	0.108	0.075	0.264	0.052	0.375	0.226	0.046	0.225	0.072	0.023
0.175	0.657	0.118	0.125	0.230	0.049	0.425	0.255	0.048	0.275	0.043	0.018
0.225	0.438	0.096	0.175	0.181	0.043	0.475	0.230	0.047	0.350	0.040	0.012
0.275	0.552	0.106	0.225	0.230	0.048	0.525	0.313	0.054	0.450	0.044	0.012
0.325	0.616	0.113	0.275	0.151	0.044	0.575	0.387	0.061	0.550	0.022	0.009
0.375	0.462	0.096	0.325	0.151	0.039	0.625	0.257	0.050	0.650	0.026	0.010
0.425	0.284	0.076	0.375	0.131	0.036	0.675	0.320	0.057	0.750	0.032	0.011
0.475	0.319	0.080	0.425	0.159	0.040	0.725	0.347	0.060	0.825	0.073	0.024
0.525	0.352	0.085	0.475	0.173	0.042	0.775	0.262	0.054	0.875	0.127	0.033
0.575	0.402	0.090	0.525	0.232	0.048	0.825	0.335	0.062	0.925	0.118	0.033
0.625	0.315	0.079	0.575	0.289	0.055	0.875	0.150	0.043	0.975	0.209	0.046
0.675	0.500	0.100	0.625	0.213	0.046	0.950	0.090	0.026			
0.725	0.276	0.074	0.675	0.236	0.049						
0.775	0.484	0.097	0.725	0.238	0.050						
0.825	0.394	0.088	0.775	0.476	0.070						
0.875	0.487	0.097	0.825	0.343	0.061						
0.925	0.361	0.085	0.875	0.503	0.074						
0.975	0.439	0.094	0.925	0.526	0.080						
			0.975	0.691	0.112						
845 Events			1118 Events			532 Events			518 Events		

Table 5
Λ polarization in the reaction $K^-p \to \Lambda\pi^0$

cos θ	P	ΔP
P_{K^-} = 862 MeV/c		
-0.950	-0.172	0.267
-0.850	0.266	0.326
-0.750	0.085	0.314
-0.650	0.111	0.349
-0.550	0.692	0.378
-0.450	-0.436	0.461
-0.350	-0.031	0.482
-0.250	-0.829	0.501
-0.100	-0.447	0.454
0.200	0.248	0.546
0.550	-0.674	0.371
0.750	-0.575	0.420
0.850	-0.372	0.299
0.950	-0.377	0.322
P_{K^-} = 902 MeV/c		
-0.950	0.087	0.288
-0.850	0.200	0.287
-0.750	-0.063	0.326
-0.650	0.226	0.351
-0.550	0.189	0.446
-0.450	0.824	0.420
-0.350	-0.186	0.435
-0.250	0.339	0.478
-0.150	-0.578	0.524
-0.050	0.702	0.508
0.100	0.278	0.480
0.350	0.662	0.440
0.600	-0.891	0.366
0.750	-0.901	0.410
0.850	-1.286	0.270
0.950	-1.117	0.292
P_{K^-} = 960 MeV/c		
-0.950	0.123	0.284
-0.850	0.097	0.274
-0.750	0.313	0.277
-0.650	0.235	0.334
-0.550	0.325	0.347
-0.450	-0.359	0.411
-0.350	0.535	0.380
-0.250	0.863	0.353
-0.150	1.645	0.400
-0.050	0.508	0.466
0.050	0.766	0.375
0.150	0.626	0.413
0.250	1.504	0.343
0.350	1.226	0.452
0.450	0.276	0.465
0.550	-0.915	0.354
0.650	-1.032	0.374
0.750	-1.197	0.289
0.850	-0.562	0.297
0.950	-0.355	0.296

cos θ	P	ΔP
P_{K^-} = 883 MeV/c		
-0.950	-0.039	0.293
-0.850	0.404	0.315
-0.750	-0.420	0.358
-0.650	0.122	0.441
-0.550	-0.482	0.482
-0.450	-0.583	0.463
-0.300	-0.140	0.441
-0.100	0.026	0.436
0.200	0.784	0.454
0.550	-0.148	0.424
0.750	-0.661	0.372
0.850	-0.306	0.357
0.950	-0.476	0.413
P_{K^-} = 918 MeV/c		
-0.950	-0.268	0.228
-0.850	-0.287	0.247
-0.750	-0.217	0.307
-0.650	0.567	0.297
-0.550	0.439	0.375
-0.450	-0.027	0.359
-0.350	-0.241	0.382
-0.250	-0.404	0.425
-0.150	0.324	0.421
-0.050	0.792	0.391
0.050	0.732	0.480
0.150	0.618	0.494
0.250	0.562	0.479
0.400	0.003	0.448
0.550	-0.275	0.505
0.650	-0.856	0.402
0.750	-1.557	0.290
0.850	-0.970	0.249
0.950	-0.554	0.253
P_{K^-} = 971 MeV/c		
-0.950	0.363	0.234
-0.850	-0.211	0.265
-0.750	0.520	0.315
-0.650	0.261	0.309
-0.550	0.448	0.328
-0.450	0.040	0.336
-0.350	-0.091	0.365
-0.250	0.419	0.358
-0.150	0.302	0.402
-0.050	0.593	0.463
0.050	0.503	0.452
0.150	0.604	0.347
0.250	1.049	0.412
0.350	0.482	0.434
0.450	-0.337	0.427
0.550	-0.205	0.355
0.650	-0.791	0.383
0.750	-0.713	0.293
0.850	-0.886	0.287
0.950	-1.067	0.252

cos θ	P	ΔP
P_{K^-} = 888 MeV/c		
-0.950	-0.017	0.276
-0.850	-0.693	0.329
-0.750	0.108	0.362
-0.650	-0.136	0.372
-0.500	0.500	0.377
-0.300	-0.300	0.402
-0.100	0.035	0.490
0.150	0.605	0.449
0.500	0.064	0.414
0.750	-0.615	0.455
0.850	-0.453	0.331
0.950	-0.219	0.368
P_{K^-} = 936 MeV/c		
-0.950	0.382	0.212
-0.850	-0.058	0.246
-0.750	0.095	0.259
-0.650	0.326	0.256
-0.550	0.482	0.255
-0.450	-0.423	0.245
-0.350	0.175	0.327
-0.250	0.028	0.405
-0.150	0.600	0.335
-0.050	0.465	0.447
0.050	1.197	0.380
0.150	0.759	0.358
0.250	-0.000	0.548
0.350	0.533	0.427
0.450	0.188	0.435
0.550	-0.572	0.427
0.650	-0.794	0.323
0.750	-1.341	0.249
0.850	-0.983	0.233
0.950	-0.632	0.268
P_{K^-} = 1001 MeV/c		
-0.950	0.022	0.347
-0.850	0.205	0.325
-0.750	0.103	0.359
-0.650	-0.098	0.400
-0.550	0.407	0.410
-0.450	1.034	0.387
-0.350	0.808	0.468
-0.250	-0.166	0.474
-0.150	0.600	0.463
-0.050	1.151	0.410
0.100	0.770	0.402
0.250	0.548	0.506
0.350	0.515	0.489
0.450	0.222	0.473
0.550	-0.242	0.473
0.650	-0.522	0.459
0.750	-1.602	0.296
0.850	-1.176	0.341
0.950	-0.496	0.407

Table 5 (continued)
Σ^+ polarization in the reaction $K^- p \to \Sigma^+ \pi^-$

cos θ	P	ΔP
P_{K^-} = 862 MeV/c		
-0.850	-0.443	0.384
-0.600	0.695	0.397
-0.350	0.529	0.378
0.0	-0.180	0.395
0.300	-0.767	0.388
0.450	-0.861	0.388
0.550	-0.522	0.369
0.650	-0.954	0.361
0.750	-0.402	0.387
0.900	-1.156	0.316
179 Events		
P_{K^-} = 883 MeV/c		
-0.900	0.308	0.413
-0.650	0.065	0.433
-0.350	0.740	0.434
0.0	-0.377	0.452
0.350	-0.429	0.317
0.550	-0.586	0.436
0.700	-1.029	0.267
0.900	-1.084	0.295
153 Events		
P_{K^-} = 888 MeV/c		
-0.900	-0.425	0.466
-0.600	0.489	0.403
-0.150	-0.173	0.651
0.250	-0.356	0.339
0.500	-0.901	0.315
0.700	-0.995	0.302
0.900	-0.661	0.334
129 Events		
P_{K^-} = 902 MeV/c		
-0.900	0.259	0.393
-0.650	0.214	0.366
-0.200	-0.041	0.433
0.200	-0.702	0.338
0.400	-0.615	0.405
0.550	-1.110	0.354
0.650	-0.664	0.377
0.750	-0.769	0.388
0.900	-0.337	0.471
158 Events		
P_{K^-} = 918 MeV/c		
-0.900	0.851	0.332
-0.700	1.652	0.289
-0.300	0.211	0.375
0.100	-0.505	0.370
0.250	-1.595	0.365
0.350	-1.196	0.365
0.450	-0.967	0.300
0.550	-0.624	0.305
0.650	-1.113	0.295
0.750	-0.672	0.313
0.850	-1.430	0.302
0.950	-1.861	0.392
250 Events		
P_{K^-} = 936 MeV/c		
-0.900	0.331	0.380
-0.700	1.070	0.309
-0.400	0.488	0.363
-0.050	-0.757	0.373
0.150	-1.670	0.408
0.250	-0.659	0.341
0.350	-1.182	0.295
0.450	-0.831	0.265
0.550	-1.176	0.258
0.650	-0.772	0.248
0.750	-1.357	0.272
0.850	-0.182	0.352
0.950	-0.177	0.460
303 Events		
P_{K^-} = 960 MeV/c		
-0.900	0.708	0.330
-0.600	1.493	0.408
-0.200	-0.485	0.588
0.100	-1.934	0.333
0.250	-0.397	0.409
0.350	-0.575	0.357
0.450	-1.340	0.272
0.550	-0.481	0.309
0.650	-0.653	0.293
0.750	-0.890	0.263
0.900	-1.162	0.277
243 Events		
P_{K^-} = 971 MeV/c		
-0.900	1.397	0.316
-0.700	0.937	0.353
-0.400	0.772	0.376
-0.050	-1.130	0.426
0.150	-0.901	0.370
0.250	-1.145	0.378
0.350	-1.276	0.272
0.450	-1.102	0.289
0.550	-0.980	0.245
0.650	-0.676	0.274
0.750	-1.013	0.295
0.900	-1.011	0.324
256 Events		
P_{K^-} = 1001 MeV/c		
-0.900	0.861	0.364
-0.600	0.452	0.406
-0.150	0.013	0.577
0.200	-1.340	0.324
0.350	-0.988	0.264
0.450	-0.817	0.305
0.550	-1.182	0.289
0.650	-1.317	0.258
0.750	-1.397	0.324
0.900	-0.958	0.340
207 Events		

Table 6
Legendre polynomial coefficients and errors for the reaction $K^-p \to \bar{K}^0n$

P (GeV/c)	A_0	A_1	A_2	A_3	A_4	A_5	A_6	$P(\cos\theta)$	$\frac{d\sigma}{d\Omega}(\theta)$ (mb/sr)	
962	.215	-.114	.184	-.215	.216	-.078	-.032	.119	.154	1.954
	.010	.020	.028	.030	.032	.034	.036		.091	.235
883	.221	-.114	.249	-.337	.225	-.099	.033	.893	.235	2.123
	.011	.023	.032	.036	.037	.039	.042		.110	.266
888	.234	-.143	.270	-.418	.278	-.150	.033	.646	.177	2.596
	.012	.025	.035	.038	.040	.041	.046		.123	.284
902	.245	-.129	.184	-.350	.245	-.044	-.016	.606	.224	1.961
	.011	.022	.030	.033	.035	.037	.040		.096	.234
918	.225	-.114	.202	-.345	.253	-.095	-.028	.235	.154	1.945
	.009	.017	.024	.026	.027	.029	.031		.071	.183
936	.269	-.136	.201	-.365	.276	-.081	-.063	.790	.159	1.986
	.009	.017	.024	.025	.027	.029	.031		.069	.174
960	.311	-.127	.261	-.393	.349	-.070	-.052	.577	.422	2.204
	.011	.021	.030	.032	.035	.037	.040		.106	.207
971	.352	-.094	.282	-.391	.429	-.120	-.055	.238	.599	2.398
	.011	.022	.031	.033	.034	.037	.041		.119	.204
1001	.440	-.096	.506	-.573	.527	-.204	-.007	.540	1.126	3.039
	.015	.032	.044	.048	.053	.054	.059		.178	.278

Of these, (5.8) through (5.13) appear as 0-prong Λ events, (5.14) through (5.17) as 2-prong Λ events, while (5.18) and (5.19) contribute to both topologies.

The MM^2 to the Λ for all 0-prong Λ events is shown in fig. 6. For the purposes of determining the $\Lambda\pi^0$ differential cross sections and polarizations, only events which gave an acceptable $\Lambda\pi^0$ fit (χ^2 probability $\geq 1\%$) were considered. However, the normalization of the $\Lambda\pi^0$ cross sections was derived from an estimation of the number of true $\Lambda\pi^0$ events, as follows:

$$N_{\Lambda\pi^0} = N_0 + N_L + N_V - N_{\Sigma^0\pi^0} ,$$

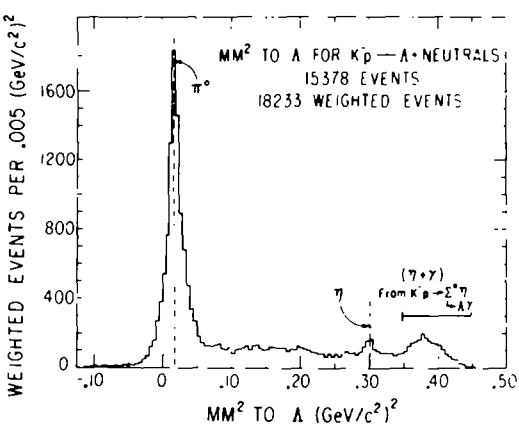

Fig. 6. Missing mass squared to the Λ for the reactions $K^-p \to \Lambda$ + neutrals. The horizontal bar indicates the overall kinematical width of the contribution from $K^-p \to \Sigma^0\eta$ from ref. [3].

Table 7
Legendre polynomial coefficients and errors for the reaction $K^- p \to \Lambda\pi^0$

P (MeV/c)	A_0	A_1	A_2	A_3	A_4	A_5	A_6	$\chi^2/(N-7)$	$d\sigma/d\Omega$ (mb/sr)	
									c	
862	.159	-.047	.275	.094	.070	.004	-.005	.590	.978	.799
	.006	.013	.017	.019	.022	.020	.021		.133	.109
895	.158	-.067	.239	.033	.042	-.035	-.070	.427	.521	.746
	.006	.014	.019	.020	.023	.022	.024		.124	.118
888	.182	-.063	.304	.053	.107	-.013	-.060	.470	.868	.546
	.007	.016	.021	.024	.027	.025	.027		.153	.136
902	.187	-.048	.269	.089	.089	-.001	-.022	.794	.919	.786
	.007	.014	.018	.021	.024	.023	.026		.136	.113
918	.180	-.038	.233	.074	.107	.006	-.012	.838	.889	.755
	.005	.011	.015	.017	.019	.019	.021		.105	.089
936	.183	-.047	.190	.045	.024	-.003	-.037	.964	.558	.572
	.005	.010	.013	.014	.017	.017	.018		.084	.072
960	.198	-.019	.177	.054	.040	.045	-.031	.524	.704	.457
	.006	.012	.015	.018	.020	.021	.023		.102	.077
971	.207	-.029	.195	.038	.077	.009	.046	.165	.807	.753
	.006	.012	.015	.018	.020	.021	.023		.099	.086
1001	.191	-.034	.130	.015	-.022	-.004	-.036	.776	.341	.403
	.007	.013	.015	.019	.022	.024	.026		.091	.084

where N_0 is the number of events in the range $-0.035 \leqslant MM^2 < 0.07$ (GeV/c^2)^2, N_L is the number of events in the range $MM^2 < 0.035$ (GeV/c^2)^2, $N_V = N_L[1 - (N_{\Sigma^0\pi^0}/(N_0+N_L))]$ is the estimated number of true $\Lambda\pi^0$ events for $MM^2 \geqslant 0.07$ (GeV/c^2)^2, $N_{\Sigma^0\pi^0}$ is the estimated number of $\Sigma^0\pi^0$ events for $MM^2 < 0.07$ (GeV/c^2)^2 using the $\Sigma^0\pi^0$ cross sections (see table 3) determined by partial-wave analysis [4].

Contaminations to $N_{\Lambda\pi^0}$ from reactions (5.10) to (5.13) were neglected because the threshold for multi π^0 production is $MM^2 \approx 0.073$ (GeV/c^2)^2, and separation of the contributions from these reactions was not attempted. The $\Lambda\eta$ cross sections in table 3 were determined from the Λ + neutrals topology by counting the events above a constant background in the range $0.28 \leqslant MM^2 \leqslant 0.32$ (GeV/c^2)^2. For a discussion of the justification of this background, see ref. [3].

The differential cross sections and Legendre polynomial coefficients for the $\Lambda\pi^0$ final state are given in table 4 (fig. 13) and table 7 respectively. The branching ratio for $\Lambda \to p\pi^-$ was taken as 0.642 [7]. The Λ polarization was measured through its decay asymmetry from the product

$$\alpha P(\cos\theta) = 3\,\frac{\sum \omega_i \cos\xi_i}{\sum \omega_i}, \tag{5.20}$$

with standard deviation

$$\Delta(\alpha P) = \left[\frac{3 - (\alpha P)^2}{N}\right]^{\frac{1}{2}}. \tag{5.21}$$

Here α is the Λ asymmetry parameter = +0.65, ξ the angle between the decay

Table 8
Associated Legendre polynomial coefficients and errors for the reaction $K^- p \to \Lambda \pi^0$

P (MeV/c)	B_1	B_2	B_3	B_4	B_5	B_6	$P(\chi^2)$
862	-.020	-.030	-.011	-.020	-.013	.009	.780
	.015	.015	.014	.012	.010	.008	
883	-.021	-.011	-.024	-.029	.000	-.006	.776
	.017	.017	.016	.013	.011	.009	
888	-.015	-.013	-.042	-.008	-.021	.014	.589
	.019	.019	.018	.015	.011	.012	
902	-.022	-.080	-.060	-.052	-.030	-.013	.660
	.018	.016	.015	.013	.011	.009	
918	-.021	-.048	-.064	-.027	-.022	.007	.332
	.014	.013	.012	.010	.009	.008	
936	.003	-.065	-.052	-.043	-.004	-.001	.420
	.014	.012	.011	.009	.008	.007	
960	.049	-.060	-.063	-.030	.008	.011	.263
	.016	.014	.013	.011	.010	.009	
971	.016	-.062	-.049	-.044	-.012	-.004	.572
	.017	.014	.013	.011	.010	.009	
1001	.030	-.077	-.067	-.029	-.011	.007	.455
	.020	.017	.014	.012	.011	.010	

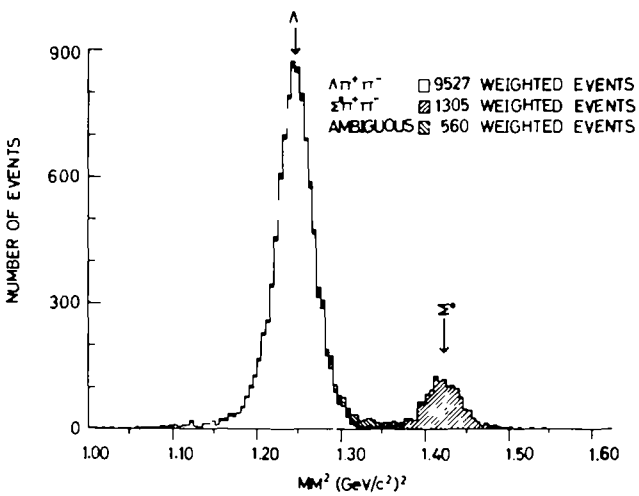

Fig. 7. Missing mass squared to the $\pi^+\pi^-$ for the reactions $K^- p \to \Lambda \pi^+ \pi^-$ and $\Sigma^0 \pi^+ \pi^-$, indicating the separation between $\Lambda \pi^+ \pi^-$ and $\Sigma^0 \pi^+ \pi^-$ events.

proton and the normal to the Λ production plane, ω_i the weight of the ith event, and N the number of unweighted events. The Λ polarizations are tabulated in table 5 and plotted in fig. 14. The associated Legendre polynomial coefficients, from the expansion

$$P(d\sigma/d\Omega) = \lambda^2 \sum_n B_n P_n^1(\cos\theta) \tag{5.22}$$

are given in table 8.

Fig. 7 is a plot of the MM^2 to the $\pi^+\pi^-$ in the 2-prong Λ reactions (5.14) and (5.15). Only a small fraction of ambiguous events is present, which were apportioned in proportion to the two populations in order to compute the cross sections for these channels in table 3. Determination of the $\Lambda\pi^+\pi^-\pi^0$ cross sections requires a rather complicated separation from reactions (5.17) and (5.19). For details of this separation and the cross sections for reactions (5.17) and (5.19), see ref. [10].

6. Charged decays

We will be concerned here mainly with $\Sigma^\pm$ decays since the greater lifetimes for

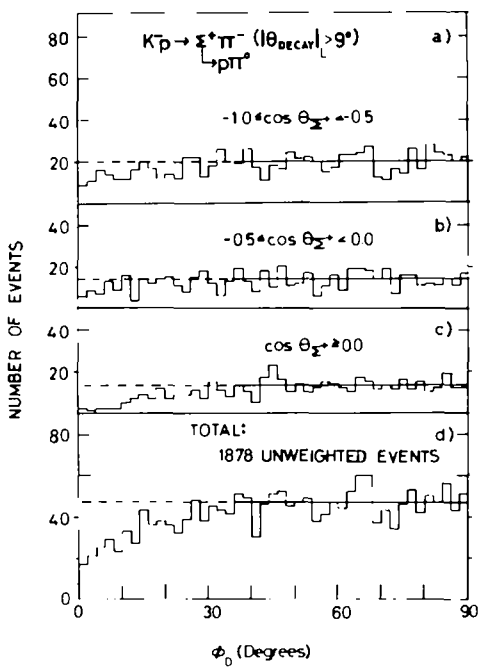

Fig. 8. Distributions of the azimuthal proton decay angle ϕ_D for $\Sigma^+ \to p\pi^0$ from events exhibiting $|\theta_{decay}|_L \geq 9°$, in different intervals of Σ c.m. production angle.

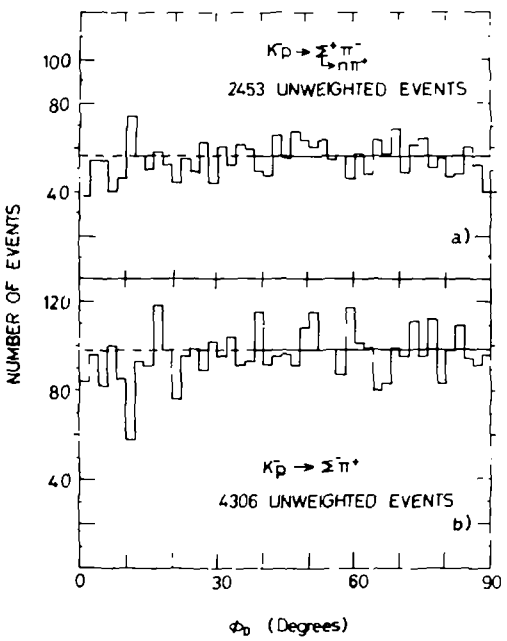

Fig. 9. Distribution of the azimuthal decay angle ϕ_D for $\Sigma^+ \to n\pi^+$ and $\Sigma^- \to n\pi^-$ decays.

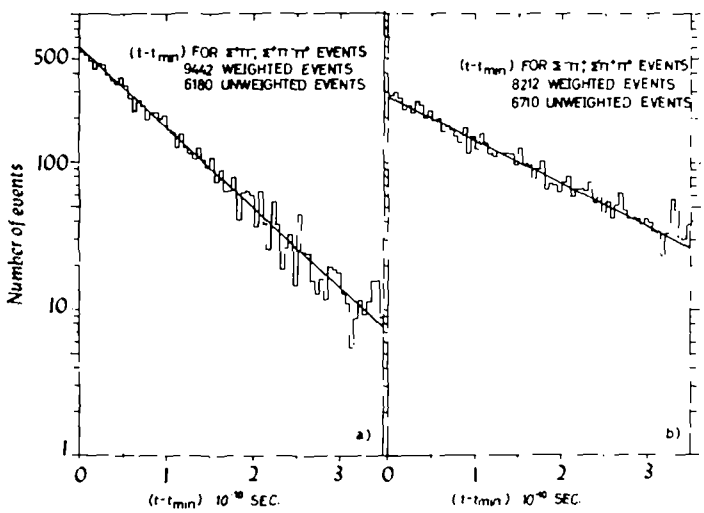

Fig. 10. (a) Distribution of the Σ^+ lifetimes, compared with the decay line for $\tau = 0.800 \times 10^{-10}$ sec [7]. t_{min} corresponds to the minimum observable lifetime, imposed by our cut-off for short Σ's. (b) Same as fig. 10(a) for Σ^- events. Here the full line is for $\tau = 1.484 \times 10^{-10}$ sec [7].

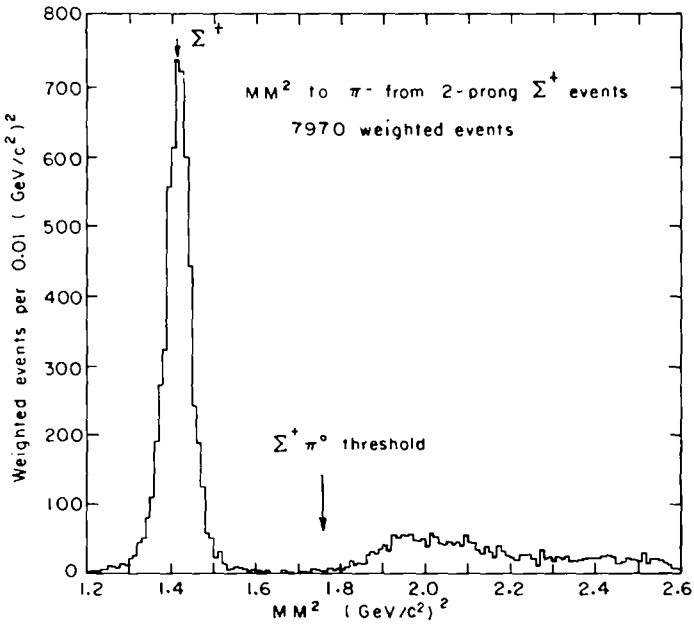

Fig. 11(a). Missing mass squared to the π^- for events of the 2-prong Σ^+ topology.

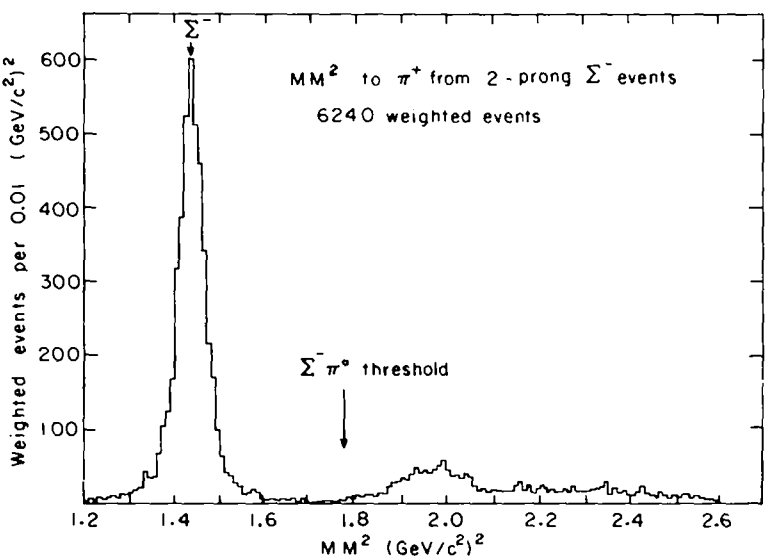

Fig. 11(b). Missing mass squared to the π^+ for events of the 2-prong Σ^- topology.

Table 9
Legendre polynomial coefficients and errors for the reaction $K^-p \to \Sigma^-\pi^+$

P (MeV/c)	A_0	A_1	A_2	A_3	A_4	A_5	A_6	$P(\cos^2)$	$\frac{d\sigma}{d\Omega}(\theta=0)$ (mb/sr)	$\frac{d\sigma}{d\Omega}(\theta=\pi)$ (mb/sr)
862	.070	-.015	.080	-.004	-.016	.024	-.011	.893	.230	.209
	.003	.007	.008	.010	.011	.011	.013		.059	.053
883	.062	-.011	.061	-.008	-.022	.036	.006	.122	.213	.153
	.003	.007	.008	.010	.011	.012	.013		.055	.051
884	.065	-.022	.075	-.002	-.034	.050	.014	.915	.300	.210
	.004	.008	.009	.011	.013	.015	.014		.065	.059
902	.070	-.019	.078	.015	-.062	.060	-.021	.197	.301	.115
	.003	.007	.009	.010	.011	.012	.013		.062	.047
918	.057	-.037	.063	.021	-.035	.051	-.023	.445	.206	.091
	.002	.005	.006	.007	.008	.009	.009		.041	.035
936	.061	-.047	.052	.033	-.021	.063	-.010	.656	.205	.049
	.002	.005	.005	.006	.007	.008	.008		.035	.027
960	.065	-.048	.062	.038	-.007	.060	-.006	.792	.244	.094
	.003	.006	.007	.008	.009	.009	.010		.042	.036
971	.072	-.059	.058	.034	-.008	.063	-.004	.296	.231	.121
	.003	.006	.007	.008	.009	.010	.010		.040	.037
1001	.085	-.067	.062	.041	-.042	.113	-.036	.729	.253	-.055
	.004	.008	.009	.010	.011	.012	.014		.052	.076

Table 10
Legendre polynomial coefficients and errors for the reaction $K^-p \to \Sigma^+\pi^-$

P (MeV/c)	A_0	A_1	A_2	A_3	A_4	A_5	A_6	$P(\cos^2)$	$\frac{d\sigma}{d\Omega}(\theta=0)$ (mb/sr)	$\frac{d\sigma}{d\Omega}(\theta=\pi)$ (mb/sr)
862	.087	.043	.045	-.045	-.069	-.048	-.001	.484	.018	.197
	.004	.008	.009	.011	.013	.015	.016		.068	.052
883	.086	.051	.061	-.032	-.058	-.031	-.021	.658	.099	.138
	.005	.009	.011	.013	.015	.017	.018		.087	.055
888	.081	.057	.053	-.021	-.072	.002	-.022	.304	.118	.021
	.005	.009	.010	.013	.016	.017	.019		.092	.049
902	.078	.036	.048	-.065	-.073	-.034	-.007	.177	-.026	.182
	.004	.008	.009	.011	.013	.014	.016		.056	.053
918	.083	.067	.050	-.059	-.073	-.007	-.013	.819	.079	.076
	.003	.007	.007	.009	.010	.011	.012		.051	.034
936	.083	.058	.052	-.073	-.058	-.017	.029	.799	.088	.187
	.003	.006	.007	.009	.010	.010	.011		.045	.037
960	.086	.072	.042	-.101	-.092	-.023	-.012	.591	-.041	.214
	.004	.007	.008	.009	.011	.012	.013		.046	.039
971	.094	.062	.036	-.115	-.092	-.014	.011	.402	-.028	.172
	.004	.007	.007	.009	.011	.012	.014		.041	.040
1001	.110	.079	.066	-.119	-.077	.015	.035	.151	.155	.225
	.005	.010	.011	.014	.015	.016	.018		.059	.055

K^- and $\pi^\pm$ make it unlikely that these particles will decay near the production vertex and simulate a $\Sigma^\pm$ event. The precautions taken in this analysis to avoid biases follow once again the approach of refs. [1,9].

(a) Weights are given to each event using eq. (5.1) to correct for the finite dimensions of the chamber and for decays occurring close to the interaction vertex. The cut-off length for the latter was $l_0 = 3.5$ mm.

(b) For $\Sigma^+ \to p\pi^0$ decays, a loss occurs when the decay proton is emitted in the

Table 11
Associated Legendre polynomial coefficients and errors for the reaction $K^- p \to \Sigma^+ \pi^-$

P (MeV/c)	B_1	B_2	B_3	B_4	B_5	B_6	$P(\chi^2)$
862	-.036	-.050	-.027	.001	-.009	.002	.626
	.012	.010	.008	.007	.006	.007	
883	-.036	-.055	-.028	-.014	-.007	-.004	.392
	.012	.011	.009	.007	.007	.006	
888	-.042	-.048	-.025	-.001	.001	.010	.994
	.013	.011	.009	.008	.008	.007	
902	-.039	-.042	-.010	.002	.010	.005	.779
	.011	.011	.009	.007	.008	.005	
918	-.055	-.091	-.013	-.016	-.008	.002	.083
	.009	.008	.007	.005	.005	.004	
936	-.056	-.067	-.005	.007	.009	.008	.165
	.008	.008	.006	.005	.004	.004	
960	-.060	-.075	-.003	-.001	-.001	-.003	.059
	.010	.009	.006	.005	.005	.004	
971	-.067	-.089	.002	-.001	.013	-.004	.896
	.010	.009	.007	.005	.005	.005	
1001	-.096	-.109	-.017	.001	.020	.001	.697
	.013	.012	.009	.008	.008	.007	

lab at a small forward angle (θ_{decay}) to the Σ^+ direction. This loss is partially corrected by requiring $|\theta_{\text{decay}}| > 9^\circ$ for these decays and weighting the accepted events. However, as is evident in fig. 8(d), there is still a significant loss for ϕ_D (eq. (5.2)) near 0°. It is also clear from fig. 8 that this loss comes more from Σ^+ produced in the forward direction (fig. 8(c)) in the c.m. than from those produced in the backward direction (figs. 8(a,b)). Therefore, the contributions to the $\Sigma^+\pi^-$ angular distributions from events with $\Sigma^+ \to p\pi^0$ decays have been weighted differently for forward (1.23) and backward (1.084) Σ^+ to correct the dependence of the loss on $\cos\theta_{\Sigma^+}$; and the contributions to the $\Sigma^+\pi^-$ and $\Sigma^+\pi^-\pi^0$ partial cross sections have been weighted by 1.122 to correct the overall loss. Finally, events with decay proton momentum $\leqslant 120$ MeV/c were rejected and the appropriate weight was assigned to the remaining events to correct this loss.

(c) The azimuthal decay distributions for $\Sigma^+\pi^-$ ($\Sigma^+ \to n\pi^+$) and $\Sigma^-\pi^+$ events are shown in figs. 9(a) and 9(b) respectively. Even without a cut on θ_{decay} for the charged pions from the Σ decays, the loss near $\phi_D = 0^\circ$ is small. A correction has been applied to the contributions to the partial cross sections by weighting $\Sigma^+ \to n\pi^+$ contributions by 1.022 and the Σ^- contributions by 1.026.

The lifetimes for Σ^+ and Σ^- events, after all cuts and corrections have been introduced, are shown in figs. 10(a) and 10(b) respectively. The decay lines for the accepted values [7] 0.800×10^{-10} sec (Σ^+) and 1.484×10^{-10} (Σ^-) are seen to fit the corrected distributions. The average weights were 1.45 for $\Sigma^+\pi^-$ ($\Sigma^+ \to n\pi^+$) events, 1.71 for $\Sigma^+\pi^-$ ($\Sigma^+ \to p\pi^0$) and 1.23 for $\Sigma^-\pi^+$ events. (Note that these aver-

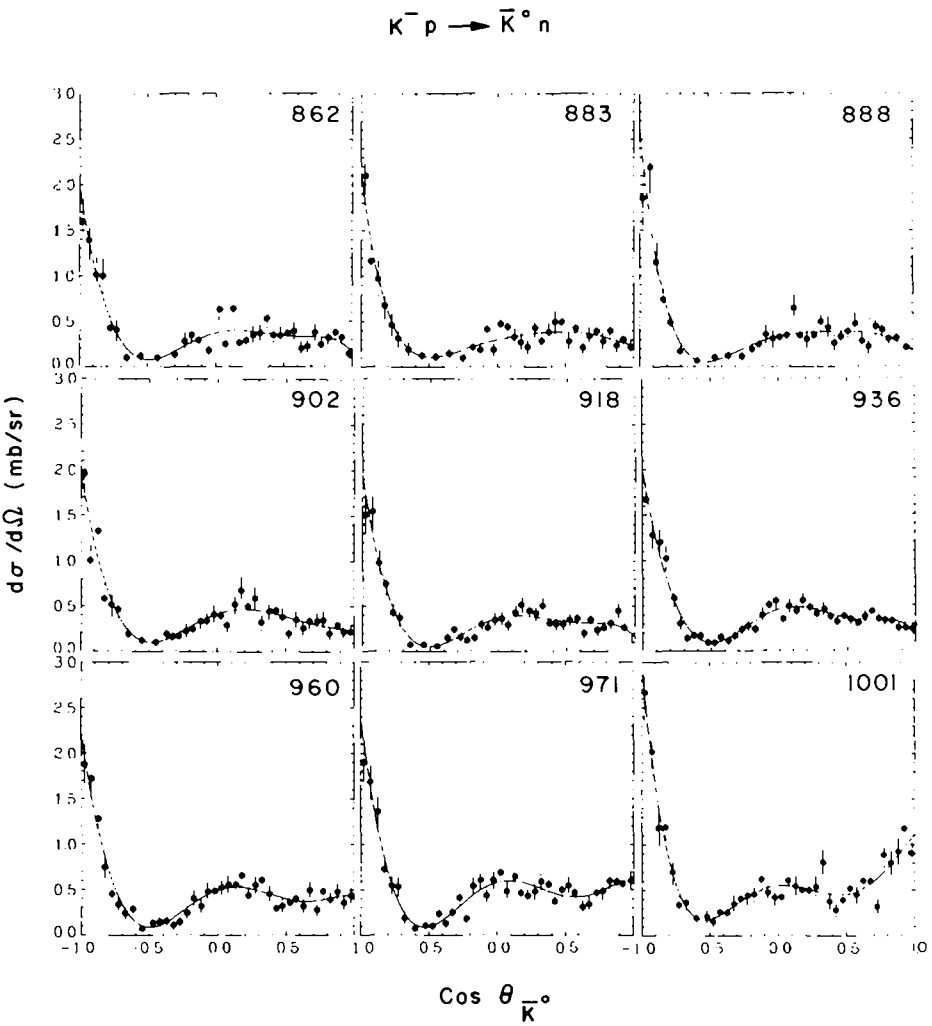

Fig. 12. Differential cross sections for the reaction $K^- p \to \bar{K}^0 n$. Shown are the data and the least-squares fit.

ages reflect only the weights assigned on an event-by-event basis and do not include the correction for the ϕ_D losses.)

The contributing $\Sigma^{\pm}$ reactions are:

$$K^- p \to \Sigma^+ \pi^- , \tag{6.1}$$

$$\to \Sigma^- \pi^+ , \tag{6.2}$$

$$\to \Sigma^+ \pi^- \pi^0 , \tag{6.3}$$

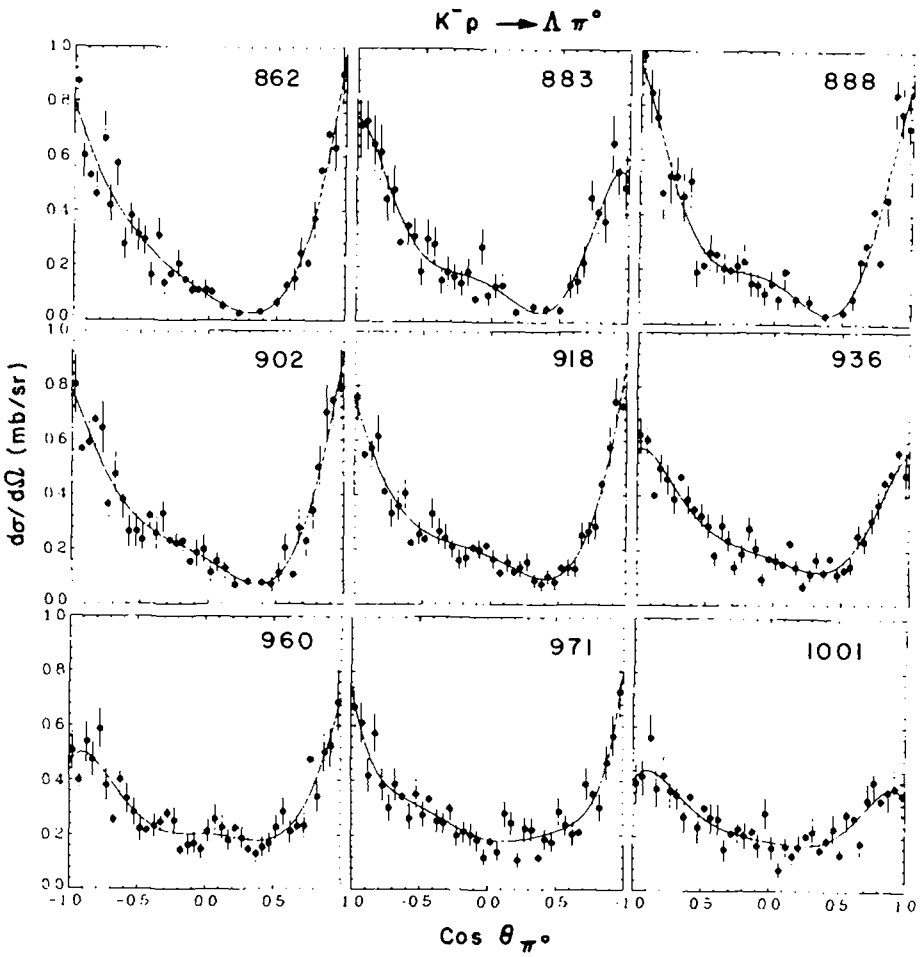

Fig. 13. Differential cross sections for the reaction $K^- p \to \Lambda \pi^0$. Shown are the data and the least-squares fit.

$$K^- p \to \Sigma^- \pi^+ \pi^0 , \tag{6.4}$$

$$\to \Sigma^+ \pi^+ \pi^- \pi^- , \tag{6.5}$$

$$\to \Sigma^- \pi^- \pi^+ \pi^+ . \tag{6.6}$$

Separation of $\Sigma^\pm \pi^\mp$ and $\Sigma^\pm \pi^\mp \pi^0$ reactions in 2-prong $\Sigma^\pm$ events was done by kinematic fitting and produced a very clean sample of $\Sigma^\pm \pi^\mp$ events (see fig. 11) for use in the determination of the differential cross sections given in table 4. The Σ^+ polarizations in table 5 were obtained from $\Sigma^+ \to p\pi^0$ decays using eq. (5.20) with

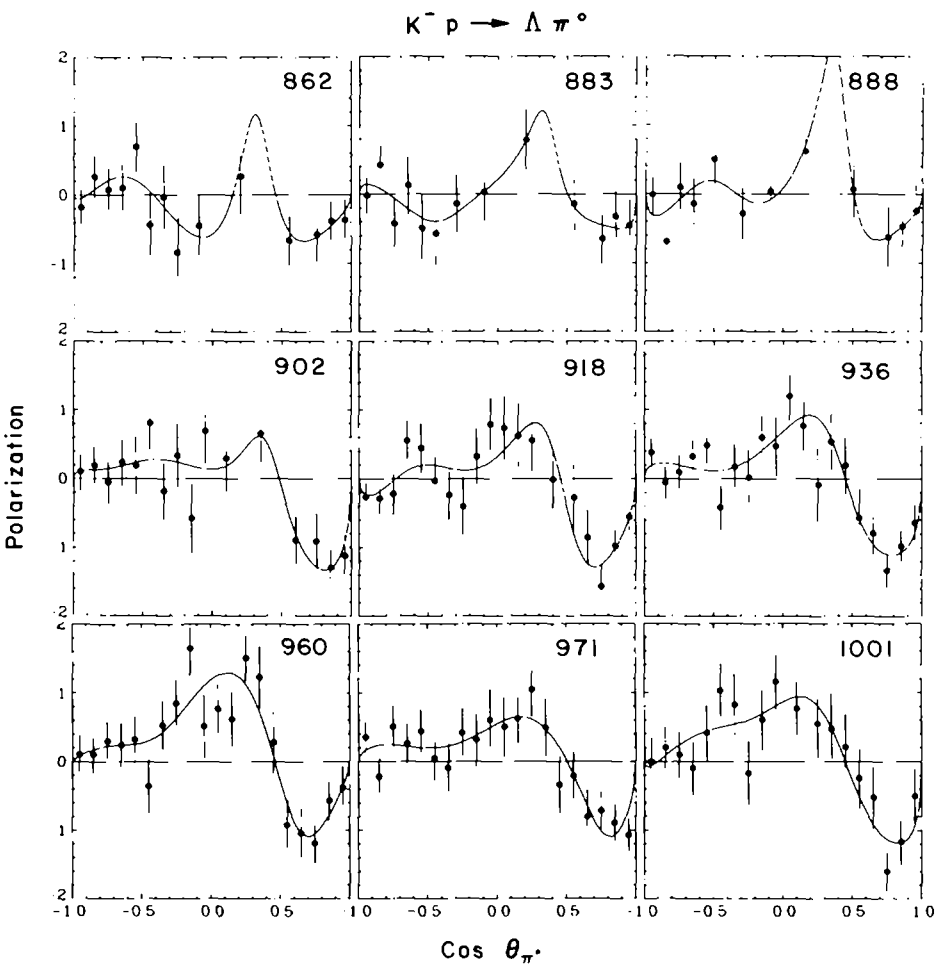

Fig. 14. Polarization of Λ in the reaction $K^-p \to \Lambda\pi^0$. Shown are the data and the least-squares fit.

$\alpha_{\Sigma_0^+} = -1.0$. Legendre and associated Legendre polynomial coefficients for these two-body final states are given in tables 9–11. Figs. 15 and 16 display the $\Sigma^-\pi^+$ and $\Sigma^+\pi^-$ angular distributions and fig. 17 shows the Σ^+ polarization. Determination of cross sections for $\Sigma^\pm\pi^\mp\pi^0$ reactions is subject to systematic problems because there is only one constraint in the kinematic fits. One problem is that $\Sigma^\pm\pi^\mp\pi^0\pi^0$ events might give acceptable fits as $\Sigma^\pm\pi^\mp\pi^0$ and thus increase the cross sections. However, judging from the numbers of observed $\Sigma^\pm\pi^\mp\pi^+\pi^-$ events (see table 1), this should be a small effect. Another problem is that there are often two acceptable solutions to the kinematic equations for $\Sigma^\pm\pi^\mp\pi^0$ fits corresponding to different values for the Σ

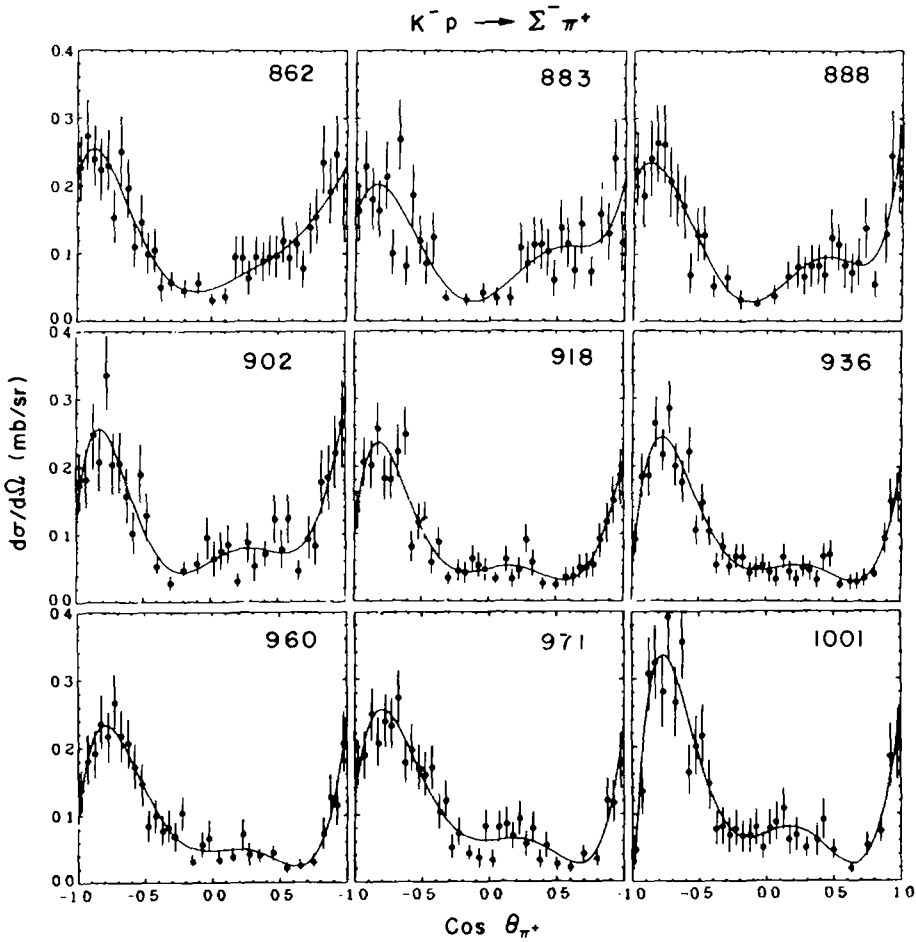

Fig. 15. Differential cross sections for the reaction $K^- p \to \Sigma^- \pi^+$. Shown are the data and the least-squares fit.

lab momentum. One solution can sometimes be rejected by checking the ionization of the Σ track, but usually the track is too short to give any significant ionization information. Since the weight of each event depends on the Σ momentum, one does not know which of the two weights to assign to a kinematically ambiguous event. Therefore, for cross-section determinations, we have given these ambiguous events the same average weight as the unambiguous $\Sigma^{\pm}\pi^{\mp}\pi^0$ events. Finally, there are often kinematic ambiguities between $\Sigma^-\pi^+\pi^0$ and $K^- p\pi^0$ or $K^-\pi^+ n$ reactions, which can simulate a Σ^- event if the K^- decays in flight. The $K^- p\pi^0$ events were easily eliminated by checking the ionization of the positive track. The $K^-\pi^+ n$ events can sometimes be eliminated by checking the negative (decaying) track ionization if this track

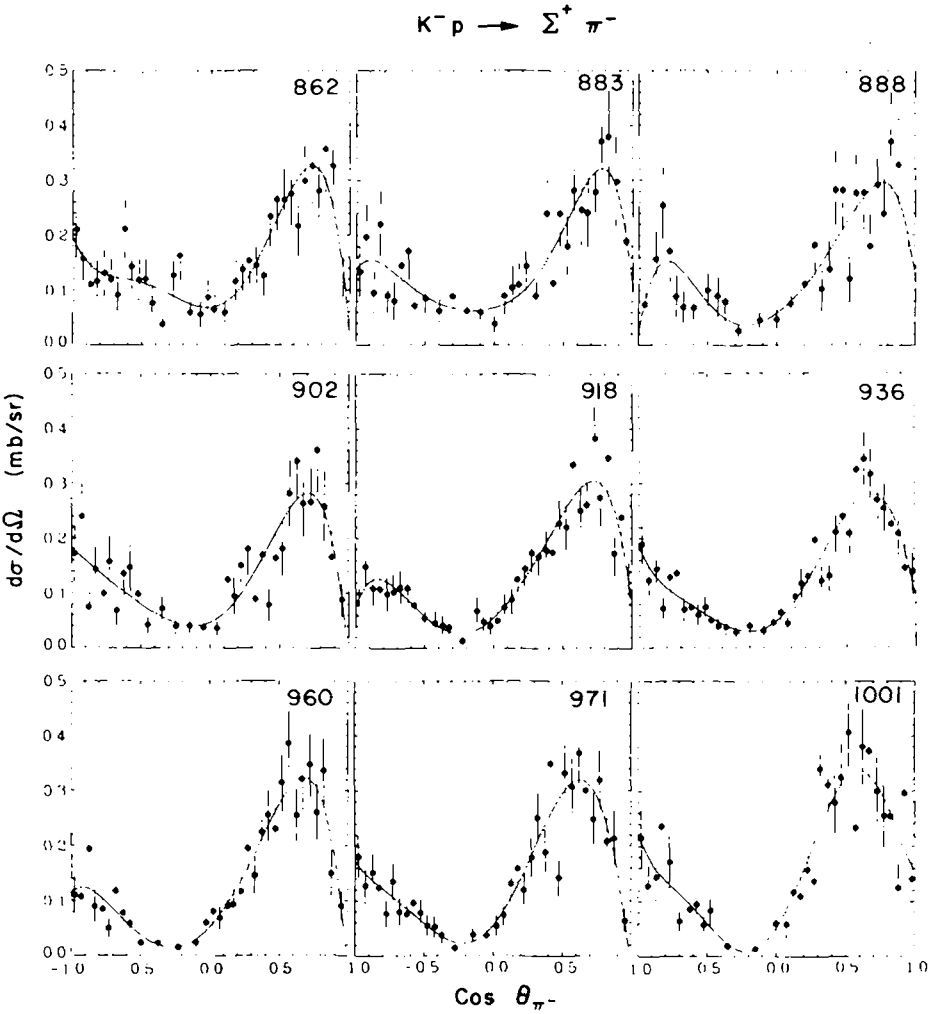

Fig. 16. Differential cross sections for the reaction $K^- p \to \Sigma^+ \pi^-$. Shown are the data and the least-squares fit.

is not too short. Because the K^- lifetime is ~ 100 times that of the Σ^-, the remaining ambiguities should contain few $K^- \pi^+ n$ events and therefore this contamination has been ignored in the calculation of $\Sigma^- \pi^+ \pi^0$ cross sections.

The successful completion of this experiment required the skill and dedication of many people both at the Enrico Fermi Institute and Lawrence Berkeley Laboratory. It is a pleasure to thank the scanning and measuring personnel, programmers, and

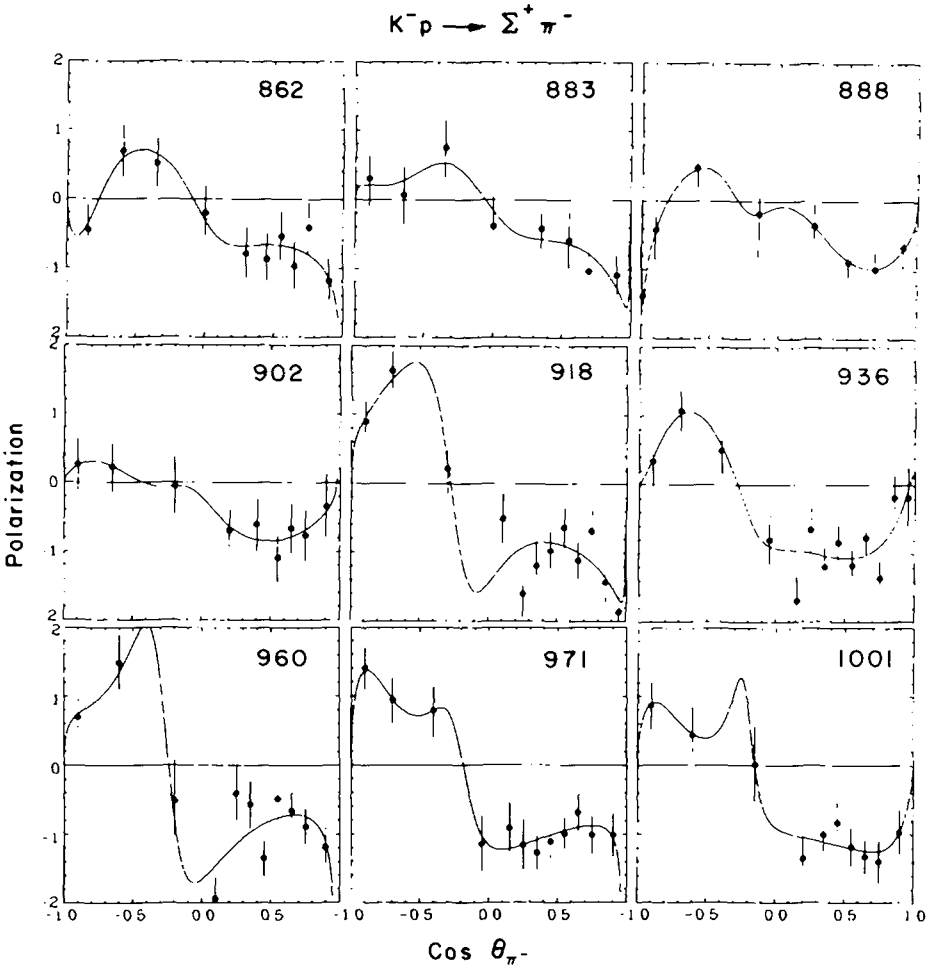

Fig. 17. Polarization of Σ^+ in the reaction $K^-p \rightarrow \Sigma^+\pi^-$. Shown are the data and the least-squares fit.

computation center staffs of both institutions; the operating crews of the Bevatron and 25" bubble chamber (R.I.P.); our colleagues at EFI, Dr. William Barletta and Dr. Bertram Schwarzschild; Dr. Frank Solmitz of LBL; and the many others whose useful contributions are often unrewarded.

References

[1] R. Armenteros et al., Nucl. Phys. B8 (1968) 233.
[2] T. Lasinski, Proc. of 16th Int. Conf. on high-energy physics, vol. 1 (1972) 60.

[3] M. Jones, Nucl. Phys. B73 (1974) 141.
[4] Chicago-LBL collaboration, Hyperon formation in the 1700 - 1900 MeV region: new data and partial-wave analysis of the $\bar{K}N$, $\Sigma\pi$, $\Lambda\pi$ channels, paper submitted to the 16th Int. Conf. on high-energy physics, Chicago, September 1972.
[5] Chicago-LBL collaboration, Multichannel partial-wave analysis of the reactions $K^-p \to \bar{K}N$, $\Lambda\pi$, $\Sigma\pi$ in the 800 - 1200 MeV/c region, paper submitted to the 1973 Meeting of the APS, Division of Particles and Fields, Berkeley, August 1973.
[6] R.B. Bell et al., UCRL-11527 (July 7, 1964).
[7] Particle Data Group, Phys. Letters 39B (1972) 1.
[8] D. Kane, Ph. D. thesis, UCRL-20682 (1971).
[9] R. Armenteros et al., Nucl. Phys. B21 (1970) 15.
[10] M. Jones, Ph.D. thesis, The University of Chicago (1974).